Published in final edited form as:
Nat Neurosci. 2013 September ; 16(9): 1248–1256. doi:10.1038/nn.3474.

Toll-6 and Toll-7 function as neurotrophin receptors in the *Drosophila* central nervous system

Graham McIlroy[1,‡], **Istvan Foldi**[1,‡], **Jukka Aurikko**[2], **Jill S. Wentzell**[1], **Mei Ann Lim**[1], **Janine C. Fenton**[1], **Nicholas J. Gay**[2], and **Alicia Hidalgo**[1,*]

[1]School of Biosciences, University of Birmingham, Edgbaston, Birmingham B15 2TT, UK

[2]Department of Biochemistry, University of Cambridge, Tennis Court Road, Cambridge, UK

Abstract

Neurotrophin receptors corresponding to vertebrate Trk, $p75^{NTR}$ or Sortilin have not been identified in *Drosophila*, thus it is unknown how neurotrophism may be implemented in insects. Two *Drosophila* neurotrophins, DNT1 and DNT2, have nervous system functions, but their receptors are unknown. The Toll receptor superfamily has ancient evolutionary origins and a universal function in innate immunity. Here we show that Toll paralogues unrelated to the mammalian neurotrophin receptors function as neurotrophin receptors in fruit-flies. *Toll-6* and *Toll-7* are expressed in the central nervous system throughout development, and regulate locomotion, motoraxon targeting and neuronal survival. DNT1 and 2 interact genetically with Toll-6 and 7, bind to Toll-7 and 6 promiscuously, and are distributed in vivo in complementary or overlapping domains. We conclude that in fruit-flies, Tolls are not only involved in development and immunity but also in neurotrophism, revealing an unforeseen relationship between the neurotrophin and Toll protein families.

Keywords

Drosophila; Toll-6; Toll-7; Toll; TLR; NFκB; neurotrophin; DNT1; DNT2; CNS; survival; axon; locomotor; neuron; receptor; HB9; Eve; Lim3

The Toll receptor superfamily comprising Toll and Toll-like receptors (TLRs) has ancient evolutionary origins, arising over 700 million years ago, and is present throughout the metazoans[1]. Toll and TLRs have a universal function in innate immunity and they initiate

*Corresponding author contact details: Phone: 00 44 (0)121 4145416 Fax: 00 44 (0)121 4145445 a.hidalgo@bham.ac.ukwww.biosciences-labs.bham.ac.uk/hidalgo.

AUTHOR CONTRIBUTIONS

G.McI., I.F., J.A., J.S.W., M.A.L, J.C.F. and A.H. performed experiments; A.H. and N.J.G. conceived and directed the project; A.H., N.J.G. and G.McI. wrote the paper; all authors contributed to planning experiments and analysing data, and to discussions and improvements to the manuscript.

‡Equal contribution first authors

Supplementary Information is linked to the online version of the paper.

AUTHOR INFORMATION

The authors declare they have no competing interests.

Europe PMC Funders Author Manuscripts

adaptive responses in vertebrates[1,2]. In humans the ten TLRs are pattern recognition receptors that directly bind to microbial antigens and activate pro-inflammatory and co-stimulatory responses. Mammalian TLRs were identified by homology to *Drosophila* Toll. The *Drosophila* genome encodes nine *Toll* receptors (*Toll-1-9*) which, except for *Toll-9*, are phylogenetically distinct from the vertebrate *TLRs*[1]. Thus, *Drosophila Toll-1* to *8* and *Toll-9* together with vertebrate TLRs form two distinct clades [3]. Toll-1 functions in developmental processes, including the establishment of the embryonic dorso-ventral axis, in axon targeting and degeneration and innate immunity[1,4], whilst the roles of the remaining Tolls are largely unresolved. Previous reports indicated that *Toll-7* to *Toll-9* have developmental functions but no antibacterial immunity functions, although *Toll-7* is involved in anti-viral responses [5-9], and *Toll-6* and *Toll-7* are expressed in the CNS[10]. Unlike the TLRs, Toll-1 does not bind microbial products directly. Instead, detection of bacterial molecules by the soluble recognition proteins PGRP and GNBP triggers a serine protease cascade[11]. This leads to the cleavage and activation of Spätzle (Spz), an endogenous protein ligand for Toll-1[12].

Spz belongs to the neurotrophin family of growth factors that in vertebrates comprises NGF, BDNF, NT3 and NT4[13,14]. Spz is comprised of a signal peptide, an unstructured pro-domain and an active cystine-knot domain of 13KDa (also known C-106), which dimerises binding Toll with 2:2 stoichiometry [13-15]. Spz is secreted as a pro-protein, and is cleaved extracellularly by the Serine proteases Easter acting in development and Spätzle Processing Enzyme (SPE) in immunity, to release the active cystine-knot[13]. This mechanism resembles the extracellular cleavage of BDNF at the synaptic cleft by the serine protease plasmin (which is also involved in the blood-clotting cascade) and which is activated by the presynaptic release of plasminogen activating factor (tPA) upon high frequency stimulation[16]. The characteristic neurotrophin cystine-knot, formed by anti-parallel β-sheets held together by three intersecting disulphide bonds, can be precisely aligned between the crystal structures of Spz and NGF[17-19].

DNT1 was identified independently as related to BDNF, using vertebrate neurotrophin sequences as query to search the *Drosophila* sequenced genome with bioinformatics tools[20]. DNT1 was found to be *spz2*, a paralogue of *spz* [20,21]. Structural prediction analysis using FUGUE showed that of the *spz* paralogues, *DNT1*and *DNT2 (spz5)*[21] are closest to the NT superfamily, followed by *spz*[21],[20].

There is also functional conservation between DNT1, DNT2 and Spz and the mammalian neurotrophins in the nervous system[20]. The vertebrate neurotrophins have essential developmental functions in neuronal survival, axon targeting and connectivity, and in adult life in learning, memory and cognition[16]. During development, *DNT1*, *DNT2* and *spz* are expressed in target cells for CNS neurons, such as the embryonic *en-passant* midline target of interneurons, and the muscles, target of motorneurons[20]. DNT1 and DNT2 are required for neuronal survival, as neuronal apoptosis decreases upon their over-expression in the CNS and it increases in the mutants leading to neuronal loss, and apoptotic neurons include HB9 and Eve positive neurons[20]. DNTs are required for motor-axon targeting, as interfering with the function of DNT1, DNT2 and Spz causes misrouting, mistargeting and sprouting defects in motoraxon terminals[20]. Thus, DNT1 and DNT2, as well as Spz, are *Drosophila*

neurotrophins based on sequence, structural and functional homology to the vertebrate neurotrophins[20].

There is further cellular and molecular evidence that neurotrophism operates in the *Drosophila* nervous system. During normal *Drosophila* development many neurons and glial cells die [22-24], and ablation or mutation in glial cells results in neuronal death in multiple contexts[25]. Identified *Drosophila* neurotrophic factors include the homologue of Mesencephalic Astrocyte-derived Neurotrophic Factor (MANF), which promotes dopaminergic neuron survival in fruit-flies using a non-canonical pathway [26] and Netrin which promotes interneuron survival from the *en-passant* midline target [27]. Gliotrophic factors of the TGF-α, neuregulin and PVF/PDGF protein families have also been shown to maintain glial survival in *Drosophila* [22,28-30].

The mammalian neurotrophins signal through three distinct receptors - $p75^{NTR}$, Trk and Sortilin - and a shared downstream target is the activation of NFκB[31-33]. In *Drosophila* there are no canonical homologues of these receptors. The receptors for DNT1 and DNT2 are unknown, although an attractive hypothesis is that orphan Tolls fulfil this function in insects. Toll receptors are generally thought to function by activating NFκB signalling, which regulates the production of antimicrobial peptides in immunity[1]. Neurotrophins also function in immunity[34], but these roles have been largely unexplored. TLRs are also present in the central nervous system (CNS), primarily in microglia, where they have immunity-related functions[35]. Thus potential relationships between the Toll and neurotrophin families may have been overlooked. Here, we ask whether Toll-6 and Toll-7 can function as receptors for DNT1 and DNT2 during CNS development.

RESULTS

Toll-6 and *Toll-7* are expressed and required in the CNS

Toll-6 and *Toll-7* are expressed in the embryonic and larval CNS, and adult central brain, as seen by mRNA patterns (Fig.1a,b,e,g,i,k). To visualise protein distribution, we used a GFP-exon trap insertion into Toll-6 (hereafter named Toll-$6^{MIMICGFP}$), and we raised anti-Toll-7 antibodies. The Toll-$6^{MIMICGFP}$ insertion is likely to result in a truncated Toll-6 protein and thus a mutant allele that could conceivably affect expression from the locus. However, we have no evidence that Toll-6 regulates its own expression. Anti-Toll-7 antibodies were found to be specific since they failed to detect signal in *Toll-7* null mutant embryos and in deficiency embryos lacking the *Toll-7* locus (Supplementary Fig.1a). In both cases, the distribution of GFP in Toll-$6^{MIMICGFP}$ and of anti-Toll-7 in wild-type matched the expression patterns of *Toll-6* and *Toll-7* transcripts, respectively (compare Fig.1a,b,e,g,i,k with Fig.1c,d,f,h,j,l). This indicates that the protein patterns most likely represent the endogenous distribution of the receptors. In Toll-$6^{MIMICGFP}$, GFP is mostly cytoplasmic whereas Toll-6 is localised to the membrane, therefore GFP does not reveal the subcellular distribution of Toll-6. Toll-$6^{MIMICGFP}$ and Toll-7 proteins are distributed in the CNS (Fig. 1c,d,f,h,j,l), including both interneurons and motorneurons (Fig.1c,d), but at this stage we cannot rule out expression also in glia. Toll-$6^{MIMICGFP}$ is present in ventral embryonic HB9+ neurons (Fig.2a); in all Eve+ motorneurons except RP2 (Fig.1c, Fig.2c,e and Supplementary Fig.2c) and in longitudinal interneuron axons (Fig.2e). Toll-7 protein is

distributed in ventral HB9+ and Lim3+ RP motorneurons (Fig.1d, Fig.2b,d and Supplementary Fig.2d), in interneuron axons that cross the midline (Fig.1d) and project along the three FasII+ longitudinal fascicles (Figs.1d and 2f), and possibly in motorneuron dendrites or perhaps glia (Fig.2d). Ventral HB9+ and Lim3+ motorneurons project along the intersegmental nerve b/d (ISNb/d), which targets to muscles 6,7,12,13. The above distributions overlap with those of GAL4 reporters for Toll-6[36] and Toll-7 (Supplementary Fig.2a,b,e-i), which include expression in the ISNb/d axonal terminals (Fig.2g). In the larva, Toll-6^{MIMICGFP} and Toll-7 are distributed along the VNC neuropile (Figs.1f,h and 2h), and Toll-6^{MIMICGFP} is detectable in aCC motorneurons (Fig.2h and Supplementary Fig.2i). In the adult brain, Toll-6^{MIMICGFP} is distributed in dopaminergic neurons (Fig.2i). Toll-6^{MIMICGFP} and Toll-7 are distributed in complementary layers of the fan-shaped body and in complementary rings of the ellipsoid body (Fig.2j), the sites for the central control of locomotion. Thus, Toll-6 and Toll-7 are distributed in the locomotor circuit, including motorneurons, interneurons of the central pattern generator, and locomotion centres and dopaminergic neurons in the brain.

To investigate the functions of Toll-6 and Toll-7 in the CNS, we generated null mutant alleles (Supplementary Fig.3). The embryonic motorneurons are preserved in the larva, thus we tracked crawling mutant larvae: most particularly, *Toll-7^{P8}/Toll-7^{P114}*; *Toll-6^{26}/Toll-6^{31}* double mutants crawled more slowly than controls (Fig. 3a,b $p<0.0001$, corrected $p<0.001$). To test whether Toll-6 and Toll-7 have functions in motor-axon targeting, we visualised the projections of FasII ISNb/d. *Toll-6^{31}/Df(3L)XG4*, *Toll-7^{P8}/Toll-7^{P114}* and *Toll-7^{114}/Df(2R)BSC22* single mutants and *Toll-7^{P8}/Toll-7^{P114}*; *Toll-6^{26}/Toll-6^{31}* double mutants showed deficient targeting and axonal misrouting (Fig. 3c,e χ^2 (7)=136.247 $p<0.001$, corrected $p<0.001$). Over-expression of constitutively active forms of the receptors, *Toll6^{CY}* and *Toll7^{CY}*, in neurons also caused targeting defects (Fig.3d,e χ^2 (7)=136.247 $p<0.001$, corrected $p=0.032$ and $p<0.001$, respectively). To test whether Toll-6 and Toll-7 can regulate cell survival, we visualised cell death with anti-cleaved-Caspase-3 antibodies and quantified the number of apoptotic cells using DeadEasy Caspase software[37]. Apoptosis increased in *Toll-6^{26}/Toll-6^{31}*, *Toll-6^{26}/Df(3L)XG4*, *Toll-7^{P8}/Toll-7^{P114}* and *Toll-7^{P8}/Df(2R)BSC22* mutant embryos, showing that Toll-6 and Toll-7 are required for cell survival in the CNS (Fig. 4a-c, (b): $F(2,70)=5.782$ $p=0.005$, corrected $p=0.006$ and $p=0.015$, respectively, and (c): $F(2,71)=7.010$ $p=0.002$; corrected, $p=0.001$ and $p=0.032$, respectively). Over-expression of *Toll-6^{CY}* and *Toll-7^{CY}* in neurons rescued naturally occurring cell death (Fig. 4d ANOVA $F(2,68)=4.811$ $p=0.011$, corrected $p=0.021$, $p=0.012$, respectively), thus Toll-6 and Toll-7 can promote cell survival. The dying cells in the double mutants included HB9+Caspase+ (Fig.4 e,f,g,h Student $t(26)=-2.230$: $p=0.035$) and Eve +Caspase+ EL interneurons (Fig.4i,j χ^2 (1)=1.992, $p=0.158$, albeit not significant), which normally express *Toll-7* and *Toll-6* (see Fig.2a-f). Not all HB9+ neurons normally express *Toll-6* or *Toll-7*, thus we could not confirm that all dying HB9+ neurons necessarily corresponded to Toll-6+ or Toll-7+ neurons. However, there was a good correlation between the ventral and central locations of the dying HB9+ neurons in the double mutants and the equivalent location of HB9+ Toll-6^{MIMICGFP} and HB9+Toll-7+ neurons in normal embryos (compare Fig.4e with Fig.2a, and Fig.4f with Fig.2b), indicating that in the mutants the HB9+ dying neurons most likely included Toll-6+ and Toll-7+ neurons. We could confirm

that since all Eve+ neurons except RP2 were also Toll-6^{MIMICGFP} positive, in the mutants apoptosis of Eve+ neurons corresponded to cell death of at least Toll-6+ neurons. Apoptosis resulted in neuronal loss as in *Toll-7^{P8}/Toll-7^{P114}*; *Toll-6^{26}/Toll-6^{31}* doubles mutants there was a reduction in the number of Eve+ EL interneurons (Fig.4k,l χ^2 (1)=9.645: p=0.002). Altogether, our data show that *Toll-6* and *Toll-7* are required for locomotion, motor-axon targeting and neuronal survival.

Toll-6 and Toll-7 interact genetically with DNT2 and DNT1

The observed CNS phenotypes resemble those caused by *DNT1* and *DNT2*[20], consistent with DNTs and Tolls being involved in common developmental processes. We next asked whether *DNT*, *Toll-6* and *Toll-7* mutants might interact genetically. Single *DNT1*, *DNT2*, *Toll-6*, or *Toll-7* mutants are viable. However, *DNT1DNT2* double mutants are semi-lethal as progeny of a heterozygous stock maintained over the *TM6B* chromosome at 18°C (Fig. 5a χ^2 (11)=360.277, p<0.001, corrected p<0.001). Similarly, *Toll-7;Toll-6* double mutant embryos are also semi-lethal at 18°C as progeny of a heterozygous stock over *SM6aTM6B* (Fig. 5a corrected p<0.001). This semi-lethality can be rescued with the expression of two forms of activated receptors in cholinergic interneurons, *Toll-6$^{\Delta LRR}$*, *Toll-7$^{\Delta LRR}$* and *Toll-7^{CY}* (Fig. 5b χ^2 (6)=85.028 p<0.001, corrected p<0.001, p=0.003, p<0.001, respectively). Exploiting this cold-sensitive semi-lethality, we tested genetic interactions between the *DNTs* and the *Tolls*. *DNT1^{41}Toll-6^{26}* and *Toll-7^{P114};DNT2^{e03444}* double mutants are semi-lethal under the above conditions, whereas *DNT2^{e03444}Toll-6^{26}* double mutant embryos are viable (Fig. 5c). The semi-lethality of *DNT1^{41}Toll-6^{26}* and *Toll-7^{P114};DNT2^{e03444}* double mutants is consistent with lack of the receptor from one signalling pathway and the ligand from the other being equivalent to losing both ligands or both receptors. The viability of *DNT2^{e03444}Toll-6^{26}* double mutants is consistent with lack of both the receptor and the ligand from the same pathway being equivalent but not worse than losing only one of them. The semi-lethality of *DNT1^{41}Toll-6^{26}* double mutants can be rescued by the over-expression of *Toll-6^{CY}* or *Toll-7^{CY}* with *Toll7GAL4* (Fig.5c χ^2 (5)=653.525 p<0.001, corrected p<0.001, p<0.001 respectively). These data suggest that Toll-7 may function downstream of DNT1 and Toll-6 downstream of DNT2. *DNT1^{41}Toll-7^{P114}* double mutants also have reduced viability, suggesting that Toll-7 may also act downstream of DNT2.

We thus asked whether activated forms of Toll-6 and Toll-7 could rescue DNT mutant CNS phenotypes. Pan-neuronal expression of *Toll-6$^{\Delta LRR}$*, *Toll-7$^{\Delta LRR}$*, *Toll-6^{CY}* or *Toll-7^{CY}* rescued the semi-lethality of *DNT1^{41} DNT2^{e03444}* double mutants (Fig.5d χ^2 (10)=401.419 p<0.001, corrected p<0.001 for all). Over-expression of *Toll-7^{CY}* in all neurons rescued the apoptosis caused by loss of *DNT1* function, and over-expression of *Toll-6^{CY}* in all neurons rescued the apoptosis caused by loss of *DNT2* function (Fig. 5e,f (e) F(2,69)=10.479 p<0.001 and (f) F(2,63)=5.143 p=0.009, and corrected p<0.01, p=0.051, p=0.011, p=0.017, respectively). Altogether, these data indicate that Toll-7 and Toll-6 most likely function as receptors for DNT1 and DNT2, respectively, although these interactions may be promiscuous.

Europe PMC Funders Author Manuscripts

Toll-6 and 7 function upstream of NFκB and bind DNT1 and 2

We next asked whether potential DNT1/2 and Toll-6/7 interactions could induce NFκB signalling. Pan-neuronal over-expression of activated *Toll*^{10b}, which activates NFκB homologues Dorsal and Dorsal-related immunity factor (Dif)[4], rescued the semi-lethality of *spz*^{2} mutants, and this rescue was replicated with the over-expression of activated *Toll-6*^{CY} and *Toll-7*^{CY} in neurons (Fig. 5g χ^2 (7)=99.272 p<0.001, corrected p<0.001, p=0.018, p<0.001, respectively). S2 cells transfected with activated *Toll-6*^{CY} and *Toll-7*^{CY} resulted in the activation, upon induction, of *snail-luciferase*, a reporter for Dorsal, and *drosomycin-luciferase*, reporter for Dif (Supplementary Fig.4a,b (a) F(5,24)=27.165 p<0.001, corrected p=0.054, p=0.000084, respectively; (b) F(5,24)=6.574 p=0.001 corrected p=0.01, p=0.018, respectively). Furthermore, when S2 cells transfected with *Toll-6HA* or *Toll-7HA*, were stimulated with purified DNT2 this triggered a *drosomycin-luciferase* readout indicative of Dif signalling (Supplementary Fig.4c,d F(5,27)=16.788 p<0.001, corrected p=0.034, p=0.09 and Supplementary Fig.5a-d). However, in vivo, over-expression of *Toll-6*^{CY} and *Toll-7*^{CY} did not induce *drosomycin-GFP* expression (Supplementary Fig.4e), consistent with previous reports[7,8]. Nevertheless, activated *Toll-6*^{CY} and *Toll-7*^{CY} induced increased levels of Dorsal, Dif and Cactus proteins (Supplementary Fig.4f Dorsal: F(2,9)=10.382, p=0.005, corrected p=0.003, p=0.085, respectively; Dif: F(2,9)=12.898, p=0.005, corrected p=0.002, p=0.006, respectively; Cactus: F(2,4.14)=28.233, p=0.004, corrected p=0.038, p=0.011, respectively). Although we do not provide mechanistic evidence of whether Toll-6 and Toll-7 signalling involve the canonical Toll pathway or not, our data indicate that Toll-6 and Toll-7 function upstream of NFκB.

In the light of the genetic evidence that Toll-6 and Toll-7 are receptors for *Drosophila* neurotrophins, we next asked whether DNT1 and DNT2 could bind Toll-7 and Toll-6. To test if they can interact in vitro, we purified secreted forms of the receptors comprising only the extracellular domain, Toll-6-ECDHis and Toll-7-ECDHis (Fig.6a,b and Supplementary Fig.5e) and cleaved baculovirus-produced DNT2-CK-His (Fig.6a,b,c Supplementary Fig.5a-d), and mixed them to allow formation of complexes which were run in a native gel (Fig. 6d,e). In native gels, protein mobility does not depend on molecular weight but on conformation and charge relative to the pH of the buffer. At the pH of our buffers both proteins were negatively charged, but the pI of DNT2CK was close to the buffer pH and its mobility was limited, whereas Toll-6/7ECDs migrated further as their pIs differed from the buffer pH. Adding DNT2-CK shifted the running of Toll-6/7ECDs and new bands appeared at the top of gel, relative to controls (Fig.6d,e). This indicates that DNT2 interacts with both Toll-6 and Toll-7.

In S2 cell culture, co-transfection with full-length *DNT1-V5* and full-length *Toll-7HA*, and *DNT2-V5* and *Toll-6HA* (Fig.6f controls), revealed interactions between DNT1 and Toll-7 and DNT2 and Toll-6 in ELISA assays (Fig.6g top 6 vs 2: t(4)=−10.485 p<0.001; 7 vs 3: t(4)=−7.619 p=0.002; bottom 7 vs 4: t(4)=−5.574 p=0.005; 6 vs 5: t(4)=−13.504 p<0.001). This interaction was also demonstrated by co-immunoprecipitation of the ligands and receptors expressed in co-transfected S2 cells. Anti-HA precipitated full-length Toll-6HA and Toll-7HA receptors, and only in receptor-transfected cells (Fig.6h control). Whereas no ligands were detected after immunoprecipitation from controls that had not been transfected

with receptors, antibodies to the HA tagged forms of Toll-6 and Toll-7 co-purified DNT2V5 and DNT1V5, respectively, from co-transfected cells (Fig.6h). There is some non-specific binding of DNT1 in the no-receptor control, but this is recurrently at lower levels than in the co-transfected cells (Fig.6h). In reverse co-IP, anti-V5 precipitated full-length and cleaved V5 tagged DNT2 and DNT1, and only in ligand-transfected cells (Fig.6i control). By contrast, no receptors were detected after immunoprecipitation from control S2 cells that had not been transfected with ligands, whereas antibodies specific for the V5 tagged forms of DNT1 and DNT2 co-purified Toll-7HA and Toll-6HA, respectively, from co-transfected cells (Fig.6i). Together, these data show that DNT1/2 and full-length transmembrane Toll-6/7 can be co-immunoprecipitated from S2 cells. In vivo, transgenic flies over-expressing both *DNT1-Cysknot-FLAG* and full-length *Toll-7HA* in the retina (with *GMRGAL4*) were used to immunoprecipitate DNT1 bound to Toll-7 (Fig.6j).

Together, these data demonstrate that DNT1 binds Toll-7 and DNT2 binds promiscuously Toll-6 and Toll-7.

Consistent with their functions as ligands for Toll-7 and Toll-6 in interneurons and motorneurons, *DNT1* and *DNT2* are expressed in embryonic CNS midline and muscle [20]. Anti-DNT1-VRY antibodies were found to be specific as they failed to reveal signal in $DNT1^{41}$ null mutant embryos (Supplementary Fig.1b). In normal embryos, DNT1 protein was detectable at the midline (Fig.7a), target of interneurons, and in high levels in muscles 13,12 and lower in muscles 6,7 - the targets of ISNb/d axons (Fig.7b). We were not able to generate a *DNT2* null allele, thus we could not confirm that anti-DNT2-KRL signal is absent in mutants. However, anti-DNT2-KRL detected ectopic DNT2 distribution in embryos, larval and adult brains (Supplementary Fig.1c-e), suggesting that it detects endogenous DNT2 protein in vivo. In normal larvae, anti-DNT2 revealed punctae along the FasII+ interneuron axons (Fig.7c), Toll-6(D42)GAL4>DsRed (Fig.7d) and Toll-$6^{MIMICGFP}$+ (Fig. 7e) axons. In adult brains, DNT1 overlies Toll-7 in fan-shaped body layers (Fig.7f), whereas DNT2 and Toll-$6^{MIMICGFP}$ are distributed in complementary layers (Fig.7f), compatible with the non-autonomous function of DNT2. Thus, the distribution of DNT1 and DNT2 supports their functioning as Toll-7 and Toll-6 ligands in vivo.

DISCUSSION

We have found that neurotrophic functions in the fruit-fly are carried out by Toll-7 and 6 binding DNT1 and 2, respectively. *Toll-6* and *Toll-7* are expressed in the locomotor circuit, including motorneurons and interneurons of the embryonic central pattern generator and locomotion centres of the adult central brain. By removing Toll-6 and Toll-7 function in mutants or adding them in excess, we have shown that Toll-6 and Toll-7 are required for normal locomotion and motoraxon targeting, and to maintain neuronal survival. In the absence of Toll-6 and Toll-7 function at least some of the dying cells are HB9+ and Eve+ EL interneurons that normally express the receptors. Using genetic interaction analysis, we have shown that Toll-6 and 7 and DNT1 and 2 function together in vivo. Using biochemical approaches in vitro, in cell culture and in vivo we have shown that Toll-6 and Toll-7 directly bind DNT2 and DNT1, respectively. Finally, the relative in vivo protein distribution patterns of the ligands and the receptors are consistent with their shared functions. Most importantly,

we have shown that Toll receptors underlie neurotrophism in fruit-flies, which is therefore implemented using a different molecular mechanism from the canonical vertebrate mechanism involving $p75^{NTR}$, Trks and Sortilin.

Our data show that Toll-6 and Toll-7 have neurotrophic functions in the Drosophila CNS matching those of DNT1 and DNT2[20]. As in the mammalian neurotrophin system, these functions are pleiotropic. Mammalian neurotrophin ligands and receptors have functions ranging from maintaining neuronal survival, to axon targeting, dendritic arborisation and synaptic transmission, which vary with context, cell type and time[16,38,39]. For instance, whereas vertebrate neurotrophins and Trk receptors maintain neuronal survival in the peripheral nervous system, they do not have a prominent role in maintaining motorneuron survival and instead have functions at the neuro-muscular junction in synaptogenesis and synaptic plasticity[40]. Our data show that Toll-6 and Toll-7 also have pleiotropic functions, maintaining predominantly interneuron survival and regulating motor-axon targeting.

Our data indicate that Toll-7/DNT1 and Toll-6/DNT2 are the most likely ligand-receptor pairs, but there appears to be promiscuity in ligand binding, since at least DNT2 can bind both receptors. This may also be the case for DNT1, but pure mature DNT1 protein could not be obtained using the baculovirus system, restricting the tests that could be carried out. Such promiscuity may account for the redundancy between Toll-6 and 7 observed in genetic and functional tests (e.g. compromised locomotion and viability in the double mutants only). It may indicate that in vivo the binding partners might be determined by the relative temporal and spatial distribution patterns of the proteins. Alternatively, it is also conceivable that DNT1 and DNT2 have distinct functions and may bind each receptor according to functional requirements. DNT1 and DNT2 have distinct biochemical properties: whereas DNT2 is consistently secreted from S2 cells as a mature, cleaved form consisting of the cystine-knot domain, DNT1 is secreted both as full-length and mature forms, and as products of cleavage within the disordered pro-domain. The protease that might cleave DNT1 in vivo is unknown, but these properties are akin to the intracellular cleavage of NGF for DNT2, and the extracellular cleavage of BDNF[16] for DNT1. In either case, the observed promiscuity is reminiscent of the binding of all mammalian neurotrophins to a common $p75^{NTR}$ receptor.

Although vertebrate neurotrophin receptors are structurally and functionally distinct from the Tolls, both regulate NFκB[1,13,32,33,41]. NFκB is also one of the transcription factors that activates the innate immune response downstream of the TLRs, and it also has extensive and highly conserved functions in neurons. Neuronal NFκB functions to control gene expression as a potent pro-survival factor, it controls neurite extension, it also has non-nuclear synaptic functions including the clustering of glutamate receptors, and it underlies synaptic plasticity during learning and memory, from crustaceans to mammals[31,32,41-43]. In humans, alterations in NFκB function lead to psychiatric disorders[41]. Previous reports have shown that Toll-6 and Toll-7 do not activate Drosomycin upon immune challenge, indicating that Toll-6 and Toll-7 do not have innate immunity functions and do not activate NFκB-Dif in cell types involved in immunity [7,8]. In future work we plan to elucidate the signalling mechanism downstream of Toll-6 and Toll-7 in the CNS and in particular to determine whether it uses downstream signal transducers such as dMyD88 that are required for the immune and

developmental functions of Toll-1. In this regard it is interesting to note that the mammalian TLR-8 is required for neurite extension in the neonatal brain but this activity is not MyD88 dependent[44]. Thus, whilst our data do not confirm or refute whether Toll-6 and Toll-7 can signal through the canonical Toll signalling pathway, they do show that Toll-6 and Toll-7 function upstream of NFκB. This conclusion is supported by several observations reported here. First, in cell culture, activated forms of Toll-6 and Toll-7 and stimulation with DNT ligands can induce NFκB signalling via Dorsal and Dif. Second, in vivo, over-expression of activated *Toll-6^{CY}* and *Toll-7^{CY}* in retinal photoreceptor neurons results in the elevation of Dorsal, Dif and Cactus proteins, as was previously reported for Toll[45]. Third, in vivo, over-expression in neurons of activated *Toll-6^{CY}* and *Toll-7^{CY}* rescues, like activated *Toll^{10b}*, the semi-lethality of *spz^{2}* mutants; and conversely, over-expression of activated *Toll^{10b}* in neurons rescues the semi-lethality of *DNT1 DNT2* double mutants. Our data also show that signalling by Toll-6 and Toll-7 differs in at least some respects from that mediated by Spz-Toll. For example, in cell culture the activation of NFκB signalling by Toll-6 and Toll-7 was not as strong as that reported by others to be induced by Toll[7,8]; and in vivo genetic rescues revealed a specific and stronger relationship between Toll-6 and 7 and DNT1 and 2, compared to Toll. Understanding the molecular mechanisms of Toll-6 and Toll-7 signalling that underlie the developmental programmes that they promote is a key objective of future research.

Intriguingly, NFκB, p75^{NTR} and Toll receptors are all evolutionarily very ancient molecules, present also in cnidarians (e.g. *Nematostella*), thus they evolved long before the common ancestor of flies and humans and since the origin of the nervous and immune systems[1,46]. Interestingly, the Toll homologue in the worm *C. elegans* is expressed in neurons and can implement an immune function via a behavioural response of pathogen avoidance[47]. p75^{NTR} is a member of the TNFR superfamily, which is closer to the Tolls than to the Trks[48]. Toll receptors resemble p75^{NTR} intracellularly, through their ability to activate a downstream signalling pathway resulting in the activation of NFκB, and Trk receptors in the extracellular ligand-binding module, with a combination of Leucin-rich (LRR) and Cys repeats[48]. Trk receptors, with an intracellular tyrosine kinase domain, emerged later in evolution[49]. Although Toll receptors are evolutionarily conserved, at least in the innate immunity context they are not activated by the same ligands in flies and humans[1]. This raises important questions: if in *Drosophila* the Trk receptors were lost and Tolls are the only neurotrophic receptors, is this a key difference that underlies the distinct brain types and behaviours in flies and humans? In the course of evolution, did the Tolls become specialised for immunity functions in vertebrates? Or is the relationship uncovered here between the neurotrophin-ligand and Toll-receptor superfamilies an ancient mechanism of nervous system formation? It is interesting to note that in mammals TLRs also have nervous system functions including in neurogenesis, neurite growth, plasticity and behaviour, but the endogenous ligands in the mammalian CNS are unknown[50]. A key objective of future research will be to investigate whether the neurotrophin and TLR protein families interact in the mammalian brain, particularly in the context of learning, memory, and neurodegenerative and neuroinflammatory diseases.

Online Methods

1.1 Genetics

Mutants and reporters—*Toll-6MiMIC*^{MI02127} is a GFP-bearing insertion into the coding region of Toll-6 (http://flybase.org/reports/FBti0140037.html). *Toll-6*^{26}, *Toll-6*^{31}, *Toll-7*^{P8} and *Toll-7*^{P114} are null mutant alleles generated by imprecise excision of P-element insertions (gift of J.L.Imler). Deficiencies *Df(3L)DXG4* and *Df(2R)BSC22* uncover *Toll-6* and *Toll-7*, respectively. *DNT1*^{41}, *DNT2*^{e03444} and *spz*^{2} have been described [20,51]. All stocks were balanced using lacZ marked balancers and/or TM6B Tb to identify mutants. Drosomycin-GFP (gift of J.M. Reihhart) is a reporter for Dif signalling.

Over-expression in vivo—Over-expression in vivo used the following GAL4 drivers: (1) *w;; elavGAL4* for all neurons; (2) *w; chaGAL4* (gift of R. Baines) for cholinergic neurons; (3) line *D42* (gift of Sanyal), for *Toll-6-GAL4* [36]; (4) *w;Toll-7GAL4*; (5) *w; GMRGAL4* (gift of Matthew Freeman) for retina; (6) *w;;HB9GAL4* for HB9-neurons; (7) *w;engrailedGAL4* (Bloomington). These were crossed to: (1) Membrane tethered reporters: (i) *w;;UASGAP-GFP* (gift of A.Chiba); (ii) *w;UASmCD8-GFP*; (iii) *w;; 10xUAS-myr-td-Tomato* (gift of B. Pfeiffer); (iv) *UASDsRed* (gift of K. Ito); (2) Activated forms of the receptors: (i) *w; UASToll-6*$^{\Delta LRR}$ and *w; UASToll-7*$^{\Delta LRR}$; (ii) *w;;UASToll-6*^{CY} and *w;;UASToll-7*^{CY} ; (iii) and w;*UASToll*^{10b} (gift of T. Ip); (iv) *w;Lim3GAL4UASmyrRFP/ CyOactYFP* (gift of M. Landgraf) . Other lines were generated by conventional genetics.

Survival Assays—Flies were bred at 18°C, as stocks or crossed from heterozygous mutants over balancer chromosomes. The survival index (SI) is given by: SI = 2 × *TM6B*$^{+}$/ *TM6B*$^{-}$. A SI of 1 is the Mendelian expectation when viability is unaffected. See Supplementary Table 1 for genotypes of parental flies and sample sizes.

1.2 Generation of fusion constructs

Toll-7GAL4—To generate *Toll-7GAL4*, a 5kb fragment immediately upstream of the *Toll-7* start ATG was amplified by PCR using primers 1, 2 (Supplementary Table 2), cloned into 5′NotI and 3′ BamHI restriction sites of the *pPTGAL* vector .

Cloning of full-length *Toll-6* and *Toll-7*—*Toll-6* and *Toll-7* are intronless genes. Full length open reading frames equivalent to cDNAs, were PCR amplified from genomic DNA, using primers 3-6 (Supplementary Table 2) and Gateway cloning was used to generate *pAct-Toll-6-HA* and *pAct-Toll-7-HA* fusion constructs.

Cloning of Toll-6ECD-His-FLAG and Toll-7ECD-His-FLAG—The extracellular domains (ECD) of Toll-6 and Toll-7 were cloned to produce secreted forms of the ligand binding domains for binding assays in vitro. Toll-6 and Toll-7ECDs sequences tagged with 6His were PCR amplified using primers 7-10 (Supplementary Table 2). Gateway cloning was used to generate *pAct-Toll-6-ECD-6His-3xFLAG* and *pAct-7-ECD-6His-3xFLAG* fusion constructs.

Generation of activated forms of Toll-6 and Toll-7 for cell culture and transgenesis—The activated Toll-6 and Toll-7 receptors; *UASToll-6$^{\Delta LRR\text{-}HA}$* and *UASToll-7$^{\Delta LRR\text{-}HA}$* are comprised of the signal peptide, transmembrane and intracellular domains of Toll-6 and Toll-7, but lack the entire extracellular domain. PCR from cDNA was used to amplify signal peptides (primers 11, 12, 15, 16 Supplementary Table 2) separately from transmembrane-intracellular domains (primers 13, 14, 17, 18 Supplementary Table 2) and MluI sites were added to each, 3′ and 5′ respectively. MluI sites were used to ligate fragments, which were then cloned into *pUAS-Gateway-HA-attB* destination vector (gift of C. Basler) to produce *pUAS-Toll-7$^{\Delta LRR}$-HA-attB* and *pUAS-Toll-6$^{\Delta LRR}$-HA-attB* fusion constructs.

In *UAS-Toll-6^{CY}* and *UAS-Toll-7^{CY}* the conserved Cysteines at position 1020 of Toll-6 and position 993 of Toll-7 are substituted for Tyrosine, mimicking the constitutively active allele of Toll, Toll^{10b}, and the functional *UASToll^{10b}* constructs. Overlap extension PCR following standard procedures was used to make the Cysteine to Tyrosine mutations in each receptor. The primers used were as follows: 5′ primers 19, 20, 23, 24 and 3′ primers 21, 22, 25, 26 (Supplementary Table 2). The resulting products were cloned into the *UAS-Gateway-FLAG* destination vector to produce *pUAS-Toll-7^{CY}-FLAG* and *pUAS-Toll-6^{CY}-FLAG* fusion constructs.

Sequencing confirmed that in *UAS-Toll-7^{CY}FLAG* and of *UAS-Toll-6^{CY}FLAG* the targeted Cysteines had been mutated to Tyrosine. There is an additional mutation in *UAS-Toll-7^{CY}FLAG* : Proline-58 to Leucine; and in *UAS-Toll-6^{CY}FLAG* : Serine-862 to Threonine, both in the extracellular domain.

Cloning for DNT protein production—DNT1 and DNT2 proteins were produced by S2 cell expression, from *pAct5C-Pro-TEV6HisV5-DNT1-CK-CTD* and *pAct5C-Pro-TEV6HisV5-DNT2-CK* fusion constructs encoding full length DNT1 and DNT2. A TEV protease sites designed to aid protein cleavage were not used, since they cleaved spontaneously. The DNT1/2 signal peptide and pro-domain were PCR amplified from DNT1/2 cDNAs, with primers 27, 28, 33, 34 (Supplementary Table 2). The DNT1/2 cystine-knots (plus the COOH extension CK-CTD for DNT1) were amplified using primers 29, 30, 35, 36 (Supplementary Table 2). Using overlapping PCR, tagged full-length DNT1/2 were obtained and cloned using *Gateway*.

To produce DNT2 protein using Baculovirus infected Sf9 insect cells, full-length DNT2 was PCR amplified from clone LD26258 (Berkeley Drosophila Genome Project) using primers 31, 32 (Supplementary Table 2). The insert was cloned into *pFastBac1* vector (Invitrogen) using EcoRI and NotI sites.

1.3 Protein purification

Purification of Toll-6ECD and Toll-7ECDs produced from S2 cells—S2 cells were transfected with *pAct-Toll-6-ECD-6His-3xFLAG* for Toll-6ECD or *pAct-7-ECD-6His-3xFLAG* for Toll-7ECD, and incubated for 72 hours. Protein purification was performed as described above for DNT1 and DNT2. Toll-6 and Toll-7 ECDs were identified by mass spectrometry, at the Proteomics Facility, University of Birmingham. Ni-NTA

purified Toll-6 and Toll-7 ECD proteins were further purified with anti-FLAG magnetic beads (Sigma-Aldrich) by standard procedures. The purified proteins were used for native gel-electrophoresis.

Purification of DNT2 produced from Baculovirus—A secreted DNT2 protein was produced in Sf9 insect cells by Baculovirus infection with *DNT2pro-CK-TEV-6xHis* sequence. The protein was purified as described previously [17]. Edman (N-terminal) Sequencing was carried out at the Protein and Nucleic Acid Chemistry (PNAC) facility at the Department of Biochemistry, University of Cambridge. The cleaved, mature cystine-knot domain of DNT2 was purified by reverse phase chromatography, as previously described for Spz[15].

1.4 Mass spectrometry

Toll-6ECD and Toll-7ECD verification—Coomassie bands were excised from gel, destained and subjected to in-gel digestion with trypsin for overnight at 37 °C using standard procedure. Peptides were extracted from gel pieces with acetonitrile and formic acid and dried in an evaporator. The samples were re-suspended in 0.1% Formic Acid/water and subjected to liquid chromatography - tandem mass spectrometry which was performed using Ultimate® 3000 HPLC series (Dionex) coupled to a LTQ Orbitrap Velos ETD mass spectrometer (ThermoFisher Scientific) via a Triversa Nanomate nanospray source (Advion Biosciences) Peptide separation, mass spectrometric analysis and database search were carried out as specified at the University of Birmingham Proteomics Facility. The LTQ Orbitrap Velos ETD mass spectrometer used in this research was obtained through the Birmingham Science City Translational Medicine: Experimental Medicine Network of Excellence project, with support from Advantage West Midlands (AWM).

DNT2 verification—DNT2CK was analysed by MALDI-TOF mass spectrometry, following procedures previously described for Spz[15].

1. 5 Western blotting

Western blotting was carried out following standard procedures. Primary antibodies used were: mouse anti-6-His (1:4000, BD Pharmingen, #552565) or mouse anti-6-His (1:1000, Thermo Scientific, #MA1-21315), mouse anti-V5 (1:5000, Invitrogen, #R960-25), mouse anti-Dorsal (7A4) (1:500, Hybridoma Bank), mouse anti-Cactus (3H12) (1:500, Hybridoma Bank), rabbit anti-Dif (1:500), chicken anti-HA (1:2000 and 1:5000, Aves, #ET-HA100), mouse anti-HA (12CA5) (1:2000, Roche, #11 583 816 001). Secondary antibodies used were: anti-mouse HRP (1:5000, Vector Labs, #PI-2000), anti-rabbit HRP (1:5000, Vector Labs, #PI-1000), anti-chicken HRP (1:10000, Jackson ImmunoResearch, #703-035-155). For quantitative analysis of dorsal, cactus and Dif expression, five adult fly heads were pooled/sample (n=4, total 20 flies/genotype), then lysed in NP-40 lysis buffer (50 mM Tris-HCl pH: 8.0, 150 mM NaCl, 1% NP-40). Western blot images were analysed by GeneTools software (Syngene). Here, band intensities were normalised to Ponceau red staining of the same membrane.

1.6 S2 cell culture signalling assays

***Toll-6* and *Toll-7* Transfections—**DNT1 was produced in S2 cells (Invitrogen) and DNT2 was produced by both S2 cells and Baculovirus. Purified ligands were added to S2 cells transfected with Toll-6 and Toll-7 receptors to test activation of the *snail-luciferase* reporter by Dorsal, or nuclear translocation of Dorsal; the cell line 648-1B6 stably transfected with *drosomycin-luciferase* was used to test the activation of the *drosomycin-luciferase* reporter by Dif. To test downstream signaling by the activated receptors, S2 were transfected with 1μg *pMTGAL4* and 1μg *pUAS-Toll-7^{CY}-FLAG* or 1μg *pUAS-Toll-6^{CY}-FLAG*. To test signaling by Toll-6 and Toll-7 upon DNT binding, full-length *Toll-6* and *Toll-7* were expressed in S2 cells by transfecting with 1μg of the *pAct-Toll-7-HA* or *pAct-Toll-6-HA* constructs. S2 cells and the S2 cell-line 648-1B6 1B6 stably transfected with *Drosomycin-Luciferase* were maintained by standard procedures and the TranIT-2020 (Mirus) transfection reagent was used. In all cases, *pAct-Renilla* was co-transfected as a control. To determine Luciferase activity, we used the Dual-Glo Luciferase Assay System (Promega). 50μl of cell suspension were transferred in triplicate to an opaque 96-well plate. 40μl of the supplied Firefly Luciferase Substrate was added, incubated for 10 minutes at room temperature, and luminescence was measured using a SPECTRAFluro Plus (Tecan). 40μl Stop & Glo substrate was added, incubated at room temperature for 10 minutes and luminescence was measured. The relative Luciferase activity was determined by normalising the Firefly over the Renilla readout for each well.

1.7 Co-immunoprecipitation (Co-IP)

In vivo Co-IP from transgenic flies—Transgenic flies of genotype *w; GMRGAL4/ UASDNT1CK3′FLAG+; UASToll-7FL-HA/+* were used for in vivo co-IP. Heads were homogenized in NP40 lysis buffer and spun at 1200g for 5 minutes at 4°. Supernatant was precleared with 20μl of protein-A/G magnetic beads (Pierce) for one hour at 4° and then incubated with 1μg mouse anti-Flag antibody (Sigma-Aldrich) overnight at 4°C. 25μl of protein-A/G magnetic beads were added to the lysate and incubated at room temperature for 1 hour. The beads containing the immuno-complex were washed twice with lysis buffer and once in PBS. The immuno-complex was eluted in 2x Laemmli-buffer by incubating for 10 mins at room temperature and was analysed by SDS/PAGE.

Co-IP from S2 cells—S2 cells were transfected with 1μg *pAct-Toll-6-HA, pAct-Toll-7-HA, pAct5C- Pro-TEV6HisV5-DNT1-CK-CTD or pAct5C-Pro-TEV6HisV5-DNT2-CK*, or co-transfected with 1μg *pAct5C- Pro-TEV6HisV5-DNT1-CK-CTD* + 1μg *pAct-Toll-7-HA* per well or 1μg *pAct5C-Pro-TEV6HisV5-DNT2-CK* + 1μg *pAct-Toll-6-HA* per well. After 48h cells were collected and spun at 1000g for 5 min at 4°C. After washing in PBS cells were lysed in 600μL NP-40 lysis buffer with protease inhibitor cocktail (Pierce Biotechnology) and left on ice for 30 min. After lysis, samples were spun at 14000g for 10min at 4°C. 500μL from each lysate was precleared with 20μL of protein-A/G magnetic beads (Pierce) for 1h at 4°C. Precleared lysates were incubated with 1.5μg anti-V5 or 1μg anti-HA antibody O/N at 4°C. Cell lysate-antibody mixtures were incubated with 25μL protein-A/G magnetic beads for 1 h at R/T. Beads were washed 2-4 times in NP-40 lysis

buffer and once in PBS. Proteins were eluted in 40 μL 2x Laemmli-buffer and analysed by SDS-PAGE.

1.8 ELISA

S2 cells were seeded, transfected and processed as described above for Co-IP. ELISA was carried out following standard procedures. High-binding capacity ELISA plate (Greiner Bio-One) wells were coated with anti-V5 antibody (1:1000) or anti-HA antibody (1:1000). Each well was incubated with 100μL of cell lysate and then with anti-HA antibody (1:1000) or anti-V5 (1:1000), respectively. ELISA signal was developed by TMB substrate (Pierce) and the reaction was stopped with 1M H_3PO_4. Absorbance was measured at 450nm.

1.9 Native gel-electrophoresis

To test if the secreted Toll-6ECD and Toll-7ECD can interact with mature DNT2-CK, proteins were mixed and putative complexes were run on a native gel. In native gels, protein mobility does not depend on molecular weight, but on conformation and charge, relative to the pH of the buffer (i.e. as the difference between the buffer pH and the pI of the proteins increases, the proteins migrate further). We used sample and gel buffers at pH=8.8 and running buffer was pH=8.6. The pI of DNT2CK-TEV-6His is pI=7.94, i.e. very close to the buffer pH. The pI of Toll6ECD-6His-3xFLAG is pI =6.06 and that of Toll7ECD-6His-3xFLAG is pI =6.0, i.e. quite different from the buffer pH. For pI and net charge calculation the Protein Calculator v3.3 was used (http://www.scripps.edu/~cdputnam/protcalc.html). At the pH of our buffers both proteins are negatively charged.

Toll-6ECD and Toll-7ECD were purified from S2 cell conditioned medium, and DNT2-CK was produced using Baculovirus and purified by reverse phase chromatography. 12.5μL Ni-NTA- and FLAG-purified Toll-6 and/or Toll-7 ECD were mixed with 2μL of reversed-phase-purified DNT2-CK and left on ice for 30 min to form complexes. Protein mixtures or proteins alone were supplemented with 4x native gel-loading buffer (62.5mM Tris-HCl pH 8.8, 20% glycerol and 0.005% bromophenol-blue). Samples were separated on a 6% polyacrylamide gel for 1h at 100V followed by 1h at 150V in the absence of SDS. Proteins were then analysed by Western blotting.

1.10 Generation of anti-Toll-7, anti-DNT1 and anti-DNT2 antibodies

Antibodies were raised to: (i) Toll-7 using peptide AAQRAQTWRPKREQLHLQQA, injected into guinea-pigs, and affinity purified (Davids Biotechnologie). (ii) DNT1: peptide VRYARPQKAKSASGEWKY; (iii) DNT2 peptide: KRLIALQGNGQN, for DNT1 and DNT2 peptides were injected into rabbits, and affinity purified (Davids Biotechnologie).

1.11 In situ hybridisations and immunohistochemistry

In situ hybridisations followed standard procedures using mRNA probes, from *pDONR-Toll-7* linearised with HindIII and *pDONR-Toll-6* linearised with SmaI, and both were transcribed with T7 RNA Pol.

Immunolabelling was carried out following standard procedures. Primary antibodies used were: rabbit anti-GFP (1:250 – 1:1000, Invitrogen #A11122), mouse anti-GFP (1:1000,

Invitrogen #A11120), rabbit anti-DsRed (1:100, Clontech #632496), mouse anti-FasII (1:4 - 1:250, DSHB ID4), mouse anti-Tyrosine Hydroxylase (TH, 1:50, Immunostar #22941), rabbit anti-cleaved-Caspase-3 (1:50, Cell Signalling #9661; 1:250 AbCam #Ab13847), mouse anti-βgal (1:750, Sigma #G4644), guinea pig anti-HB9 (1:1000, gift of H.Broihier), rabbit anti-HB9 (1:1000, gift of H.Broihier), mouse anti-Eve (1:5-1:10, DSHB 2B8), mouse anti-Dorsal (1:10, DSHB 7A4), guinea pig anti-Toll-7-AAQ (1:10 -1:30), rabbit anti-DNT1-VRY (1:50-1:100), rabbit anti-DNT2-KRL (1:50 -1:100). Secondary antibodies were directly conjugated Alexa488, 546 and 647 (1:250, Molecular Probes) or biotinylated mouse or rabbit (1:300) followed by avidin amplification using the Vectastain ABC Elite kit (Vector Labs) or Streptavidin-Alexa488 (1:250, Molecular Probes). Stainings were carried out in populations of hundreds of embryos, at least 3 adult brains and 3 larval VNCs per experiment, and experiments were repeated at least twice and most often more.

1.12 Imaging

Laser-scanning confocal microscopy was carried out using a Leica SP2-AOBS and a 40x or 63x lens at 512×512 or 1024×1024 pixels resolution, with 0.5 or 1 μm steps. Caspase+ apoptotic cells in vivo were counted automatically using DeadEasy Caspase software[37].

1.13 Automatic tracking of larval locomotion

Larvae were collected from crosses kept in vials with standard yeast-rich food at 25°C in 12h Light:12h Dark regime. All larvae analysed were also homozygous *white (w)* mutant. For our w^+ *Toll-6*^{26} stock, to obtain *w; Toll-6*^{31}*/Toll-6*^{26} larvae, F1 larvae from a cross to *w; Toll6*^{31} females were sexed and only w^- males were used. Larvae were collected, rinsed in water and placed on a large petri-dish containing agar, Vogel-Bonner salts and 40% glucose at room temperature, and on a light box. Larvae were allowed to recover for 10-20 seconds before filming commenced, and were then filmed for 1 minute. All filming was carried out in the morning between 1-5 hours after zeitgeber 'lights on' time and larvae from all genotypes were filmed in each session. Larvae were filmed using a Motic MC Camera 1.1 or a Cannon viedo camera.

Films were analysed using FlyTracker software (our modification of the ImageJ MTrack2 plug-in). Cannon films were first converted to .avi format using Any Video Converter Professional with codec .mjpeg and Motic films were decompressed using VirtualDub software (www.virtualdub.org) and saved in .avi format. Films were checked in VirtualDub for sequence continuity and images not containing larvae were edited out to ensure a continuous sequence of filmed crawling larvae. The first 400 frames were opened blindly in ImageJ, converted to greyscale, the resolution was set to 800 × 600 pixels, and saved as a stack of .tiff images. These were next analysed using FlyTracker in ImageJ. FlyTracker tracks the crawling larvae and produces three outputs per film: a stack of 400 images with the location of the larva as identified by the software in each corresponding raw image; a path or trajectory of each larva in each film as a single .jpeg image; an excel spreadsheet with quantitative locomotion parameters. The speed in mm/sec was converted from the output in pixels using a photographed reference of known size in mm. All trajectories for each genotype were plotted onto a single image using Adobe Photoshop layers.

1.14 Statistical analysis

For continuous data, kurtosis, skewness, histograms and Kolmogorov-Smirnov normality tests were carried out to test data distribution, and Levene tests for the homogeneity of variance. For a few samples that were not distributed normally within a data set that showed normal distribution, normality was assumed. Normally distributed data were analysed with unpaired t-tests for two sample comparisons, and One Way ANOVA (or Welch versions for significant Levene tests) for the whole data set followed by Dunnett (fixed control group) or Games-Howell (significant Levene tests) post-hoc tests or Bonferroni corrections for multiple t-tests. Data that were not distributed normally were analysed with Kruskal-Wallis for the whole data set followed by Dunn's test for multiple comparisons. Categorical data were analysed with Chi-square tests, followed by a z-test and Bonferroni post-hoc to the whole data set or Bonferroni corrections for pairwise comparisons to controls. No blinding was done. For genetic in vivo experiments, the reproducibility of the experiment was verified by the overall large population sizes; cell culture experiments were carried out in general at least three times in triplicate. P values, tests and sample sizes are provided in the Results text and figure legends and further details in Supplementary Table 3.

Supplementary Material

Refer to Web version on PubMed Central for supplementary material.

ACKNOWLEDGEMENTS

We thank C. Arnot, J. Wen and M. Wheatley for advice, S. Jondhale, J.Ng and S. Quayle for technical help, S.Bishop and K.Kato for comments on the manuscript and A.J. Courey, J.L.Imler, T. Ip, J.M.Reichhart, the Bloomington Stock Centre and Iowa Hybridoma Bank for reagents, the Birmingham Mass Spectrometry Facility (Birmingham Science City, Advantage West Midlands), and Len Packman for mass spectrometry and Edman sequencing in Cambridge. This work was funded by MRC-Career Establishment Grant to A.H., Wellcome Trust Project Grant to A.H. and N.G., WT Equipment Grant to A.H., WT Programme Grant to N.G., EU Marie Curie International Incoming Fellowship to J.S.W., MRC studentship to G.McI and Brunei Government Studentship to M.A.L.

REFERENCES

1. Leulier F, Lemaitre B. Toll-like receptors--taking an evolutionary approach. Nat Rev Genet. 2008; 9:165–178. doi:nrg2303 [pii]10.1038/nrg2303. [PubMed: 18227810]
2. Janeway CA Jr. Medzhitov R. Innate immune recognition. Annu Rev Immunol. 2002; 20:197–216. doi:10.1146/annurev.immunol.20.083001.084359 [pii]. [PubMed: 11861602]
3. Imler JL, Zheng L. Biology of Toll receptors: lessons from insects and mammals. J Leukoc Biol. 2004; 75:18–26. doi:10.1189/jlb.0403160 [pii]. [PubMed: 12960276]
4. Lemaitre B, Nicolas E, Michaut L, Reichhart JM, Hoffmann JA. The dorsoventral regulatory gene cassette spatzle/Toll/cactus controls the potent antifungal response in Drosophila adults. Cell. 1996; 86:973–983. doi:S0092-8674(00)80172-5 [pii]. [PubMed: 8808632]
5. Yagi Y, Nishida Y, Ip YT. Functional analysis of Toll-related genes in Drosophila. Dev Growth Differ. 2010; 52:771–783. doi:10.1111/j.1440-169X.2010.01213.x. [PubMed: 21158756]
6. Nakamoto M, et al. Virus recognition by Toll-7 activates antiviral autophagy in Drosophila. Immunity. 2012; 36:658–667. doi:S1074-7613(12)00094-5 [pii] 10.1016/j.immuni.2012.03.003. [PubMed: 22464169]
7. Tauszig S, Jouanguy E, Hoffmann JA, Imler JL. Toll-related receptors and the control of antimicrobial peptide expression in Drosophila. Proc Natl Acad Sci U S A. 2000; 97:10520–10525. doi:10.1073/pnas.180130797 [pii]. [PubMed: 10973475]

8. Ooi JY, Yagi Y, Hu X, Ip YT. The Drosophila Toll-9 activates a constitutive antimicrobial defense. EMBO Rep. 2002; 3:82–87. doi:10.1093/embo-reports/kvf004 [pii]. [PubMed: 11751574]
9. Seppo A, Matani P, Sharrow M, Tiemeyer M. Induction of neuron-specific glycosylation by Tollo/Toll-8, a Drosophila Toll-like receptor expressed in non-neural cells. Development. 2003; 130:1439–1448. [PubMed: 12588858]
10. Kambris Z, Hoffmann JA, Imler JL, Capovilla M. Tissue and stage-specific expression of the Tolls in Drosophila embryos. Gene Expr Patterns. 2002; 2:311–317. doi:S1567133X02000200 [pii]. [PubMed: 12617819]
11. Hoffmann JA. The immune response of Drosophila. Nature. 2003; 426:33–38. doi:10.1038/nature02021[pii]. [PubMed: 14603309]
12. Weber ANR, et al. Binding of Drosophila cytokine Spatzle to Toll is direct and establishes signaling. Nature Immunology. 2003; 4:794–800. [PubMed: 12872120]
13. Gay NJ, Gangloff M. Structure and function of Toll receptors and their ligands. Annu Rev Biochem. 2007; 76:141–165. doi:10.1146/annurev.biochem.76.060305.151318. [PubMed: 17362201]
14. DeLotto Y, DeLotto R. Proteolytic processing of the Drosophila Spatzle protein by easter generates a dimeric NGF-like molecule with ventralising activity. Mech. Dev. 1998; 72:141–148. [PubMed: 9533958]
15. Gangloff M, et al. Structural insight into the mechanism of activation of the Toll receptor by the dimeric ligand Spätzle. J Biol Chem. 2008; 283:14629–14635. [PubMed: 18347020]
16. Lu B, Pang PT, Woo NH. The yin and yang of neurotrophin action. Nat Rev Neurosci. 2005; 6:603–614. doi:nrn1726 [pii] 10.1038/nrn1726. [PubMed: 16062169]
17. Arnot CJ, Gay NJ, Gangloff M. Molecular mechanism that induces activation of Spatzle, the ligand for the Drosophila Toll receptor. J Biol Chem. 2010; 285:19502–19509. doi:M109.098186 [pii] 10.1074/jbc.M109.098186. [PubMed: 20378549]
18. Hoffmann A, et al. Biophysical characterization of refolded Drosophila Spatzle, a cystine knot protein, reveals distinct properties of three isoforms. J Biol Chem. 2008; 283:32598–32609. doi:M801815200 [pii]10.1074/jbc.M801815200. [PubMed: 18790733]
19. Hoffmann A, Neumann P, Schierhorn A, Stubbs MT. Crystallization of Spatzle, a cystine-knot protein involved in embryonic development and innate immunity in Drosophila melanogaster. Acta Crystallogr Sect F Struct Biol Cryst Commun. 2008; 64:707–710. doi:S1744309108018812 [pii] 10.1107/S1744309108018812.
20. Zhu B, et al. Drosophila neurotrophins reveal a common mechanism for nervous system formation. PLoS Biol. 2008; 6:e284. doi:08-PLBI-RA-0237 [pii] 10.1371/journal.pbio.0060284. [PubMed: 19018662]
21. Parker JS, Mizuguchi K, Gay NJ. A family of proteins related to Spatzle, the toll receptor ligand, are encoded in the Drosophila genome. Proteins Struct., Function Genet. 2001; 45:71–80.
22. Jacobs JR. The midline glia of Drosophila: a molecular genetic model for the developmental functions of glia. Progress in Neurobiology. 2000; 62:475–508. [PubMed: 10869780]
23. Rogulja-Ortmann A, Lüer K, Seibert J, Rickert C, Technau GM. Programmed cell death in the embryonic central nervous system of Drosophila melanogaster. Development. 2007; 134:105–116. [PubMed: 17164416]
24. White K, et al. Genetic control of programmed cell death in Drosophila. Science. 1994; 264:677–683. [PubMed: 8171319]
25. Hidalgo A, et al. Trophic neuron-glia interactions and cell number adjustments in the fruit fly. Glia. 2011; 59:1296–1303. doi:10.1002/glia.21092. [PubMed: 21732425]
26. Palgi M, et al. Evidence that DmMANF is an invertebrate neurotrophic factor supporting dopaminergic neurons. Proc Natl Acad Sci U S A. 2009; 106:2429–2434. doi:0810996106 [pii]10.1073/pnas.0810996106. [PubMed: 19164766]
27. Newquist G, et al. Blocking apoptosis signaling rescues axon guidance in Netrin mutants. Cell Reports. 2013; 3:1–12. [PubMed: 23219549]
28. Bergmann A, Tugentman M, Shilo BZ, Steller H. Regulation of cell number by MAPK-dependent control of apoptosis: a mechanism for trophic survival signaling. Dev. Cell. 2002; 2:159–170. [PubMed: 11832242]

29. Hidalgo A, Kinrade EFV, Georgiou M. The Drosophil Neuregulin Vein maintains glial survival during axon guidance in the CNS. Developmental Cell. 2001
30. Learte AR, Forero MG, Hidalgo A. Gliatrophic and gliatropic roles of PVF/PVR signaling during axon guidance. Glia. 2008; 56:164–176. doi:10.1002/glia.20601. [PubMed: 18000865]
31. Gutierrez H, Davies AM. Regulation of neural process growth, elaboration and structural plasticity by NF-kappaB. Trends Neurosci. 2011; 34:316–325. doi:S0166-2236(11)00038-5 [pii]10.1016/j.tins.2011.03.001. [PubMed: 21459462]
32. Foehr ED, et al. NF-kappa B signaling promotes both cell survival and neurite process formation in nerve growth factor-stimulated PC12 cells. J Neurosci. 2000; 20:7556–7563. doi:20/20/7556 [pii]. [PubMed: 11027214]
33. Carter BD, et al. Selective activation of NF-kappa B by nerve growth factor through the neurotrophin receptor p75. Science. 1996; 272:542–545. [PubMed: 8614802]
34. Levi-Montalcini R, Aloe L, Alleva E. A role for Nerve Growth Factor in nervous, endocrine and immune systems. Progress in NeuroEndocrinImmunology. 1990; 3:1–10.
35. Rivest R. Regulation of innate immune responses in the brain. Nat Rev Immunol. 2009; 9:429–439. [PubMed: 19461673]
36. Sanyal S. Genomic mapping and expression patterns of C380, OK6 and D42 enhancer trap lines in the larval nervous system of Drosophila. Gene Expr Patterns. 2009; 9:371–380. doi:S1567-133X(09)00025-8 [pii]10.1016/j.gep.2009.01.002. [PubMed: 19602393]
37. Forero MG, Pennack JA, Learte AR, Hidalgo A. DeadEasy caspase: automatic counting of apoptotic cells in Drosophila. PLoS One. 2009; 4:e5441. doi:10.1371/journal.pone.0005441. [PubMed: 19415123]
38. Huang EJ, Reichardt LF. Trk receptors: roles in neuronal signal transduction. Annu Rev Biochem. 2003; 72:609–642. doi:10.1146/annurev.biochem.72.121801.161629 [pii]. [PubMed: 12676795]
39. Blum R, Konnerth A. Neurotrophin-mediated rapid signaling in the central nervous system: mechanisms and functions. Physiology (Bethesda). 2005; 20:70–78. doi:20/1/70 [pii]10.1152/physiol.00042.2004. [PubMed: 15653842]
40. Liu X, Jaenisch R. Severe peripheral sensory neuron loss and modest motor neuron reduction in mice with combined deficiency of brain-derived neurotrophic factor, neurotrophin 3 and neurotrophin 4/5. Dev Dyn. 218:94–101. doi:10.1002/(SICI)1097-0177(200005) 218:1<94::AID-DVDY8>3.0.CO;2-Z [pii] 10.1002/(SICI)1097-0177(200005). [PubMed: 10822262]
41. Mattson MP, Meffert MK. Roles for NF-kappaB in nerve cell survival, plasticity, and disease. Cell Death Differ. 2006; 13:852–860. doi:4401837 [pii] 10.1038/sj.cdd.4401837. [PubMed: 16397579]
42. Freudenthal R, Romano A. Participation of Rel/NF-kappaB transcription factors in long-term memory in the crab Chasmagnathus. Brain Res. 2000; 855:274–281. doi:S0006-8993(99)02358-6 [pii]. [PubMed: 10677600]
43. Heckscher ES, Fetter RD, Marek KW, Albin SD, Davis GW. NF-kappaB, IkappaB, and IRAK control glutamate receptor density at the Drosophila NMJ. Neuron. 2007; 55:859–873. doi:S0896-6273(07)00616-2 [pii] 10.1016/j.neuron.2007.08.005. [PubMed: 17880891]
44. Ma Y, et al. Toll-like receptor 8 functions as a negative regulator of neurite outgrowth and inducer of neuronal apoptosis. J Cell Biol. 2006; 175:209–215. doi:jcb.200606016 [pii] 10.1083/jcb.200606016. [PubMed: 17060494]
45. Reichhart JM, et al. Expression and nuclear translocation of the rel/NF-kappa B-related morphogen dorsal during the immune response of Drosophila. C R Acad Sci III. 1993; 316:1218–1224. [PubMed: 8062131]
46. Putnam NH, et al. Sea anemone genome reveals ancestral eumetazoan gene repertoire and genomic organization. Science. 2007; 317:86–94. doi:317/5834/86 [pii] 10.1126/science.1139158. [PubMed: 17615350]
47. Pujol N, et al. A reverse genetic analysis of components of the Toll signaling pathway in Caenorhabditis elegans. Curr Biol. 2001; 11:809–821. doi:S0960-9822(01)00241-X [pii]. [PubMed: 11516642]
48. Bothwell M. Evolution of the neurotrophin signaling system in invertebrates. Brain Behav Evol. 2006; 68:124–132. doi:94082 [pii]10.1159/000094082. [PubMed: 16912466]

49. Sossin WS. Tracing the evolution and function of the Trk superfamily of receptor tyrosine kinases. Brain Behav Evol. 2006; 68:145–156. doi:94084 [pii]10.1159/000094084. [PubMed: 16912468]

50. Okun E, Griffioen KJ, Mattson MP. Toll-like receptor signaling in neural plasticity and disease. Trends Neurosci. 2011; 34:269–281. doi:S0166-2236(11)00021-X [pii]10.1016/j.tins.2011.02.005. [PubMed: 21419501]

REFERENCE APPEARING ONLY IN METHODS

51. Weber AN, Gangloff M, Moncrieffe MC, Hyvert Y, Imler JL, Gay NJ. Role of the Spatzle Pro-domain in the generation of an active toll receptor ligand. J Biol Chem. 2007; 282:13522–13531. doi:M700068200 [pii] 10.1074/jbc.M700068200. [PubMed: 17324925]

Europe PMC Funders Author Manuscripts

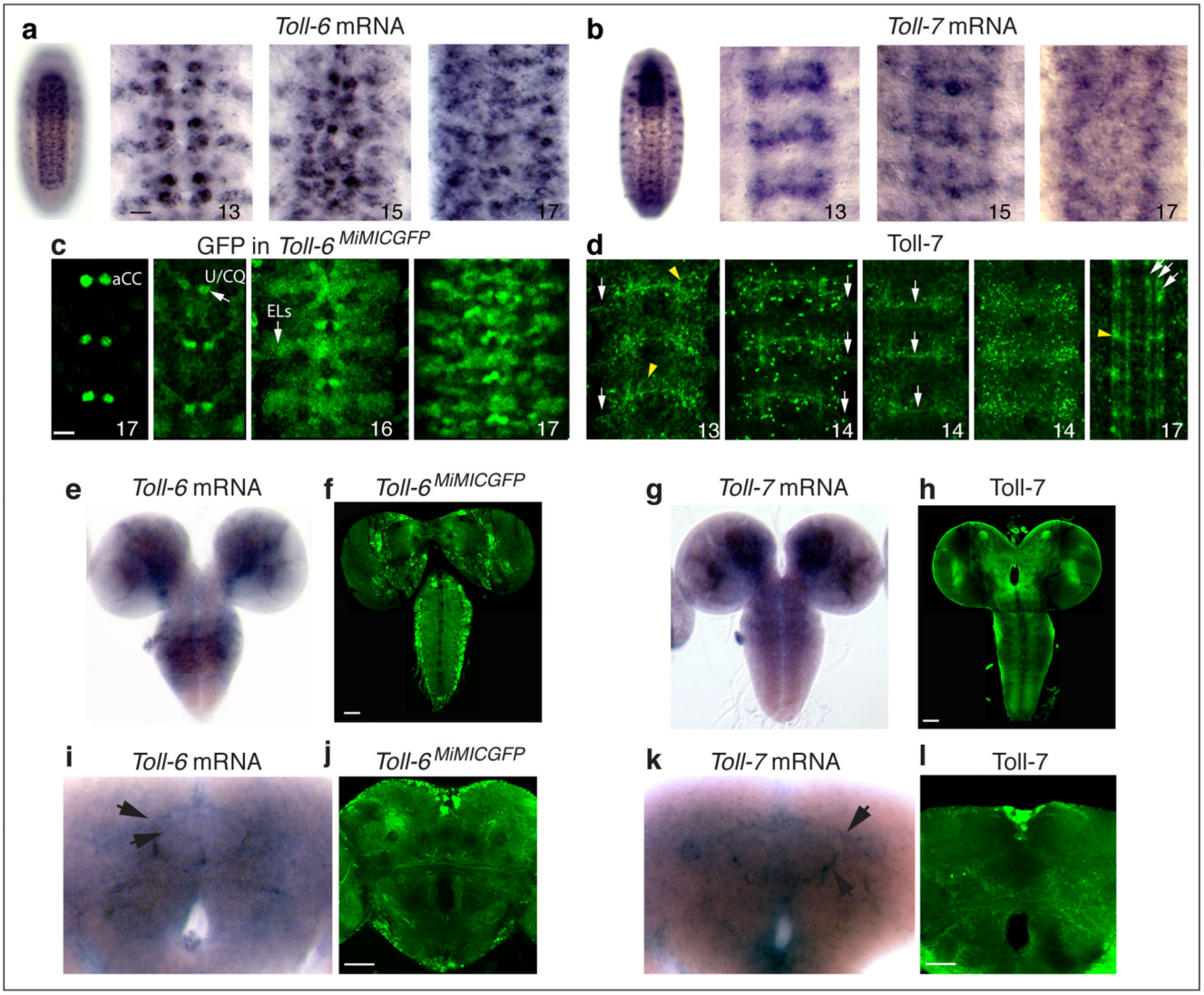

Fig.1. *Toll-6* and *Toll-7* are expressed in the CNS through all stages

In situ hybridisations showing transcripts for *Toll-6* and *Toll-7* in: (a,b) stage 13, 15 and 17 embryos; (e,g) larval optic lobes, central brain and ventral nerve cords; (i,k) adult brain in central complex (arrows). (c,d,f,h,j,l) Distribution of GFP in Toll6^{MIMICGFP} and anti-Toll7 matches that of the transcripts. (c) Note GFP signal in distinct neuronal types (arrows); (d) Note motoraxons exiting the CNS (first and second image, white arrows), motorneuron cell bodies (yellow arrowheads), axons crossing the midline (third image, arrows), and along three interneuron fascicles (fifth image, arrows), and in thickenings that might correspond to dendrites or glia (yellow arrowhead). (i,k) Note signal in and around fan shaped body. EL, U/CQs: Eve neurons. Anterior is up. Scale bar in: (a,c) 10 μm; (f,h,j,l) 50 μm.

Europe PMC Funders Author Manuscripts

Europe PMC Funders Author Manuscripts

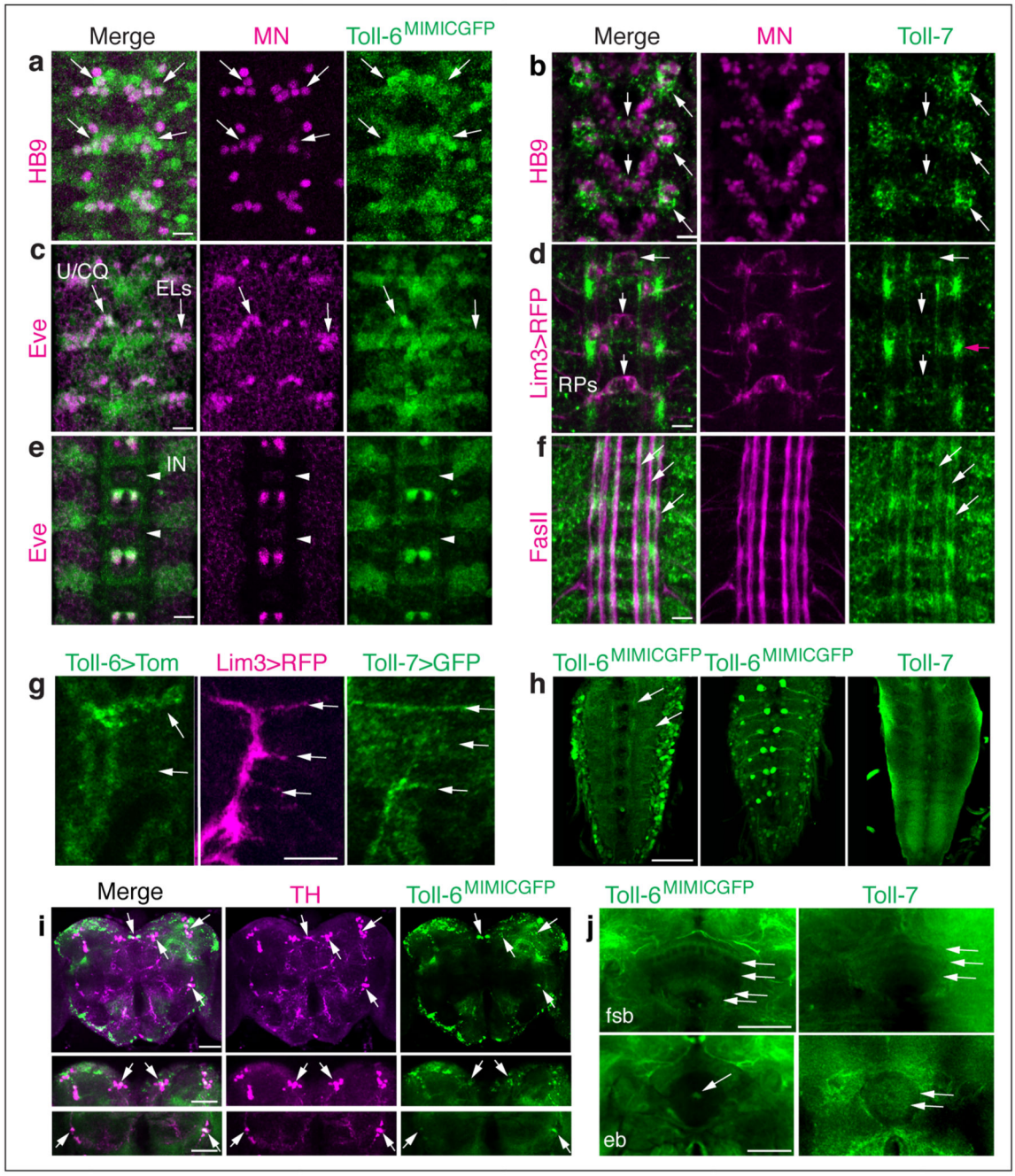

Fig. 2. Identification of Toll-6 and Toll-7 cells in the locomotor circuit

(a,c,e) Anti-GFP in Toll6^{MIMICGFP} embryos is distributed in ventral lateral nerve cord HB9+ neurons (a), Eve+ EL interneurons and all Eve+ motorneurons except RP2 (c,e, arrows, for RP2s see Supplementary Fig.2c). IN=interneurons, arrowheads pointing at longitudinal connectives. (b,d,f) Toll-7 protein is localised to ventral lateral and medial HB9+ neurons (b, arrows), Lim3GAL4>myrRFP+ RP motorneurons (d, arrows) and possibly dendrites (pink arrow) and FasII+ interneuron fascicles (f, arrows). (g) Toll-6GAL4 (D42)>10xmyr-tdTomato and Toll-7GAL4>GAPGFP reveal ISNd/b terminals (compare to

Lim3GAL4>myrRFP). (h) Toll6^{MIMICGFP} and Toll-7 are present in the larval VNC neuropile (arrows pint at axons) and at least Toll6^{MIMICGFP} in motorneurons. (i) Toll6^{MIMICGFP} colocalises with the dopamine precursor Tyrosine Hydroxylase (TH) in most dopaminergic neurons. (j) Toll6^{MIMICGFP} and Toll-7 are distributed in distinct layers of the fan-shaped body (fsb, arrows) and rings of the ellipsoid body (eb, arrows). Scale bars: (a-g) 10μm, (h-j) 50μm.

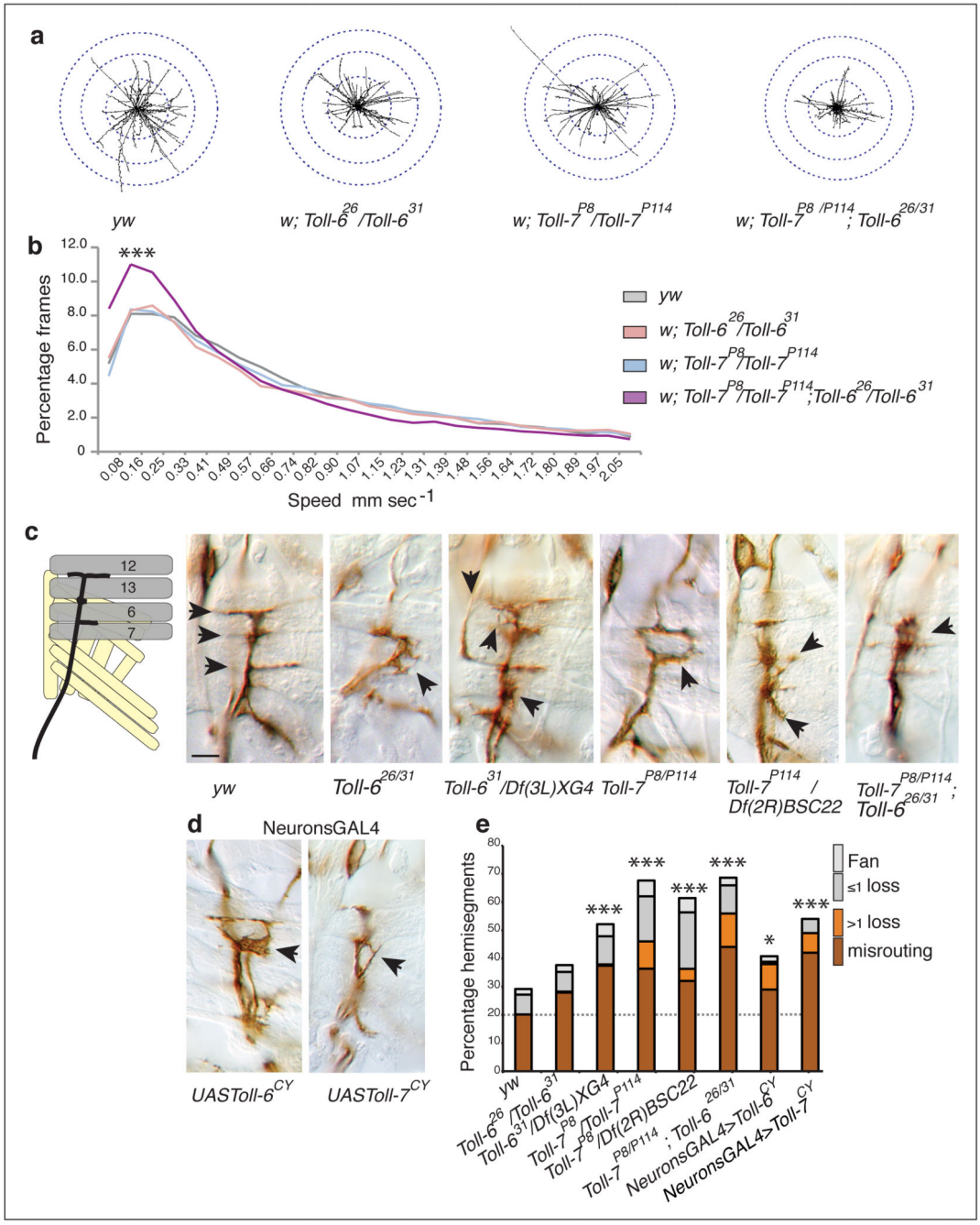

Fig. 3. Toll-6 and Toll-7 are required for larval locomotion and motor-axon targeting

(a) Trajectories of larvae crawling for 400 frames per larva, n=50 larvae per genotype . (b) *Toll-7 Toll-6* double mutant larvae crawl more slowly. Kruskal-Wallis 814: p<0.0001, and Dunn's test for pair-wise comparisons, asterisks refer to double mutants vs. *yw* controls (Dunn=4474), n=50 larvae and 19950 frames per genotype. (c-e) The incidence of FasII+ motoraxon misrouting in 1 or more projections, and loss of two or more projections, per hemisegment increase in (c,e) stage 17 mutant embryos and (d,e) embryos over-expressing activated forms of *Toll-6* or *Toll-7* in all neurons (elavGAL4>Toll-6^{CY};Toll-6^{CY} and

Toll-7GAL4;elavGAL4>Toll-7^{CY}). Scale bar: 10 μm. (e) Chi-Square χ^2 (7)=136.247 p<0.001, pair-wise comparisons to *yw* Chi-square with Bonferroni correction, n=169-465 hemisegments per genotype. *p<0.05; ** p<0.01; ***p<0.001. For further details see Supplementary Table 3.

Europe PMC Funders Author Manuscripts

Europe PMC Funders Author Manuscripts

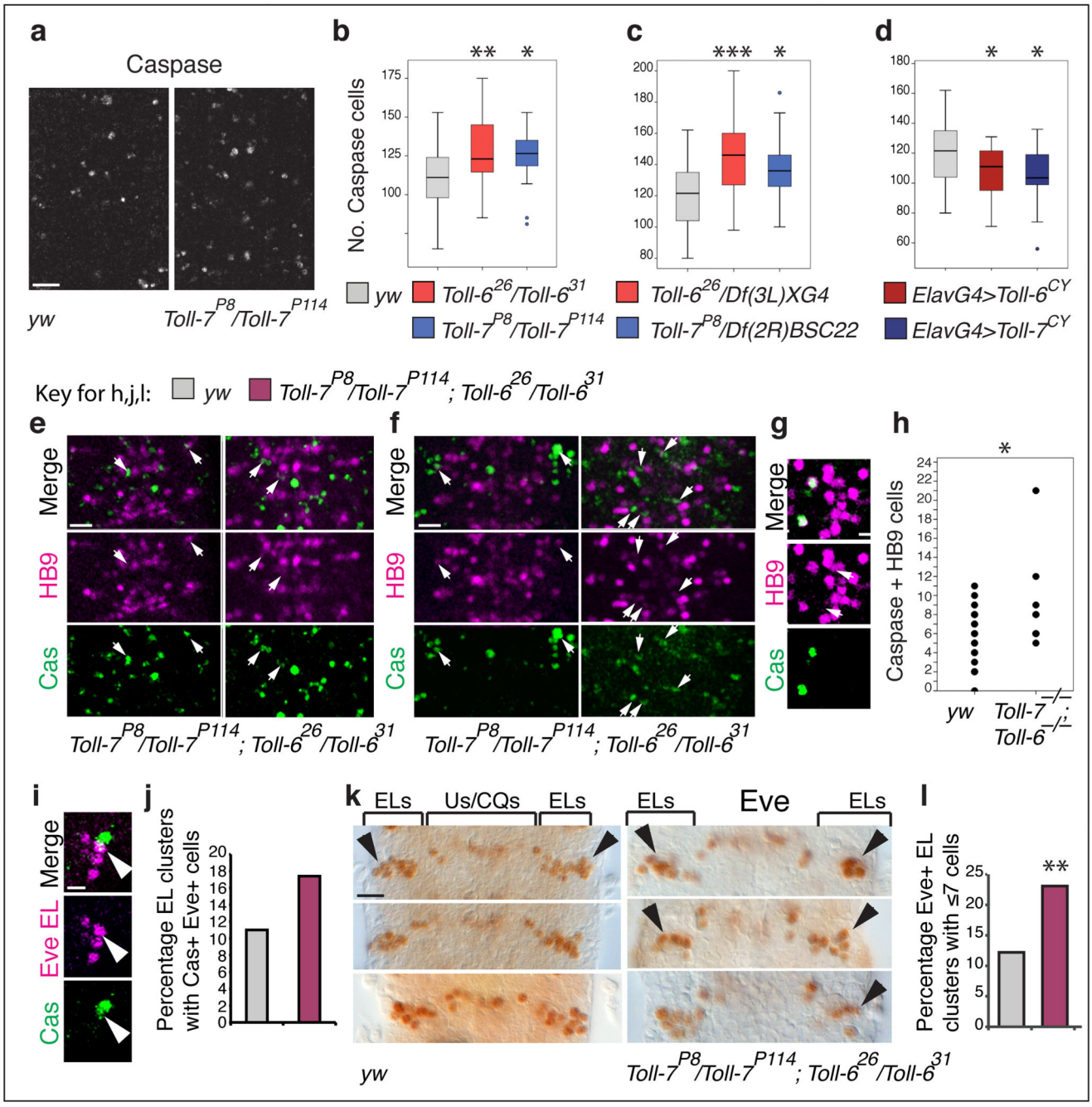

Fig. 4. Toll-6 and Toll-7 maintain neuronal survival

(a) Embryonic VNCs labelled with anti-cleaved-Caspase-3. (b,c) Apoptosis increases in *Toll-7* and *Toll-6* mutant embryos, as quantified with DeadEasy software: (b) One Way ANOVA $F(2,70)=5.782$: $p=0.005$, post-hoc Dunnett $p=0.006$, $p=0.015$, respectively, n=19-28 embryos per genotype; (c) One Way ANOVA $F(2,71)=7.010$ $p=0.002$, post-hoc Dunnett $p=0.001$, $p=0.032$, respectively, n=21-31 embryos. (d) Pan-neuronal over-expression of *activated Toll-6* and *Toll-7* rescues naturally occurring cell death in the CNS, One Way ANOVA $F(2,68)=4.811$ $p=0.011$, post-hoc Dunnett $p=0.021$, $p=0.012$,

respectively, n=22-27 embryos. (b-d) Asterisks refer to pair-wise comparisons to *yw*, post-hoc Dunnett tests. (e-h) Apoptotic Caspase+HB9+ cells in *Toll7^{P8}/Toll7^{P114}; Toll6^{26}/Toll6^{31}* double mutant embryos in locations corresponding to neurons that normally express (e) *Toll-6* or (f) *Toll-7*, (g) high magnification view and (h) quantification, unpaired Student t-test (1)=−2.230, p=0.035, n=9-19 embryos. (i,j) In *Toll7^{P8}/Toll7^{P114}; Toll6^{26}/Toll6^{31}* double mutant embryos, more EL clusters have Eve+ Caspase+ apoptotic interneurons (j, albeit not significant $\chi^2(1)=1.992$ p=0.158, n=109-138 EL clusters). (k,l) Apoptosis leads to loss of Eve+ EL interneurons in the double mutants, as more EL clusters have fewer neurons than the normal 8-10 per cluster (arrows in k), Chi-square $\chi^2(1)=9.645$ p=0.002, n=22-260 EL clusters. *p<0.05; **p<0.01;***p<0.001. All stage 17 embryos. Scale bars: (a) 20 μm; (e, f, k) 10 μm; (g, i) 5 μm. For further details see Supplementary Table 3.

Europe PMC Funders Author Manuscripts

Europe PMC Funders Author Manuscripts

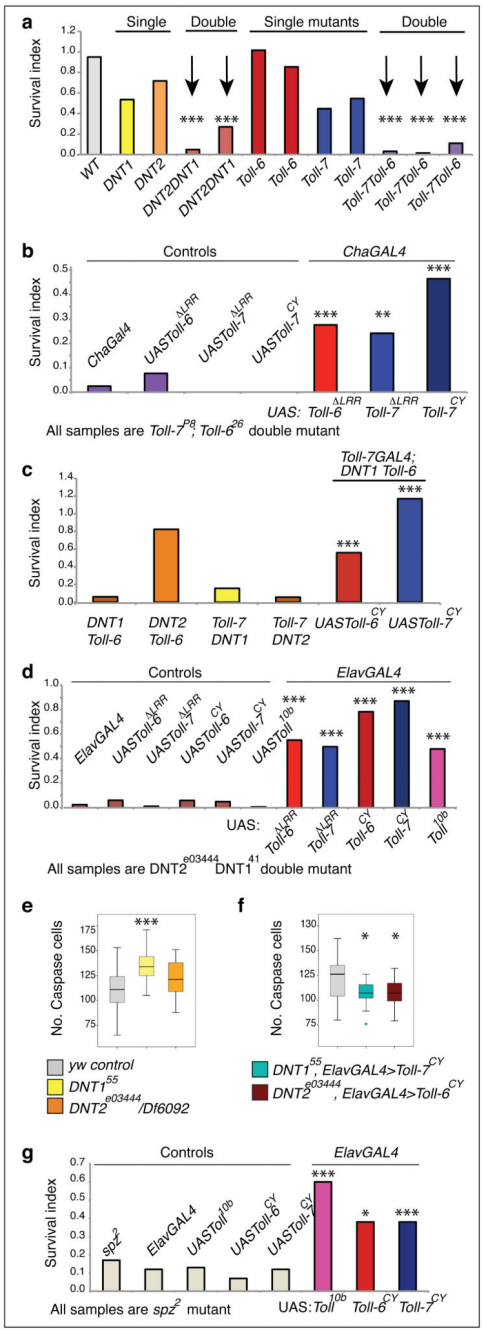

Fig. 5. Toll-6 and Toll-7 interact genetically with DNT2 and DNT1

Survival index for homozygous *yw;;*+/+ controls bred from an outcross to *TM6B* at 18°C is 1. (a) Single homozygous mutants lacking one *DNT* or *Toll-6* or *Toll-7* are viable, whereas homozygous double mutants lacking *DNT1* and *DNT2* or *Toll-6* and *Toll-7* are semi-lethal if bred at 18°C as progeny of a stock maintained over a *TM6B* or *SM6aTM6B* balancer. Chi-square $\chi^2(11)=360.277$ $p<0.001$, n=126-872 pupae per genotype. (b) The semi-lethality of $Toll\text{-}7^{P8};Toll\text{-}6^{26}$ double mutants can be rescued by over-expressing the activated receptors in cholinergic neurons. $\chi^2(6)=85.028$ $p<0.001$, n=102-467 pupae. (c) Homozygous double

mutants lacking one *DNT* and one *Toll* recapitulate the semi-lethality of $DNT1^{41}DNT2^{e03444}$ and $Toll\text{-}7^{P8};Toll\text{-}6^{26}$ double mutants, and the lethality *DNT1 Toll-6* double mutants can be rescued by expressing the activated receptors with *Toll-7GAL4*. $\chi^2(5)=653.525$ $p<0.001$, n=72-991. (d) The semi-lethality of $DNT1^{41}DNT2^{e03444}$ double mutants can be rescued by expressing the activated *Toll-6, Toll-7* or *Toll* receptors in neurons. $\chi^2(10)=401.419$ $p<0.001$, n=83-1461 pupae. (e,f) Quantification of anti-cleaved-Caspase-3 labelling in embryonic VNCs: apoptosis increase of DNT^{55} and $DNT2^{e03444}/Df6092$ mutant embryos (e, One Way ANOVA $F(2,69)=10.479$ $p<0.001$, post-hoc Dunnett $p<0.01$, $p=0.051$) is rescued with the over-expression of activated $Toll\text{-}7^{CY}$and $Toll\text{-}6^{CY}$ in all neurons (f, Welch ANOVA $F(2,63)=5.143$ $p=0.009$, post-hoc Dunnett $p=0.011$, $p=0.017$). (e,f) Asterisks refer to pairwise comparisons to *yw*, post-hoc Dunnett tests. (g) Pan-neuronal over-expression of activated $Toll^{10b}$, $Toll\text{-}6^{CY}$ and $Toll\text{-}7^{CY}$ rescues the semi-lethality of spz^2 mutants, $\chi^2(7)=99.272$ $p<0.001$. ***$p<0.001$; **$p<0.01$; *$p<0.05$. (a-d,g) Asterisks refer to Chi square comparisons to fixed controls with Bonferroni corrections. For detailed genotypes and further statistics details, see Supplementary Tables 1 and 3.

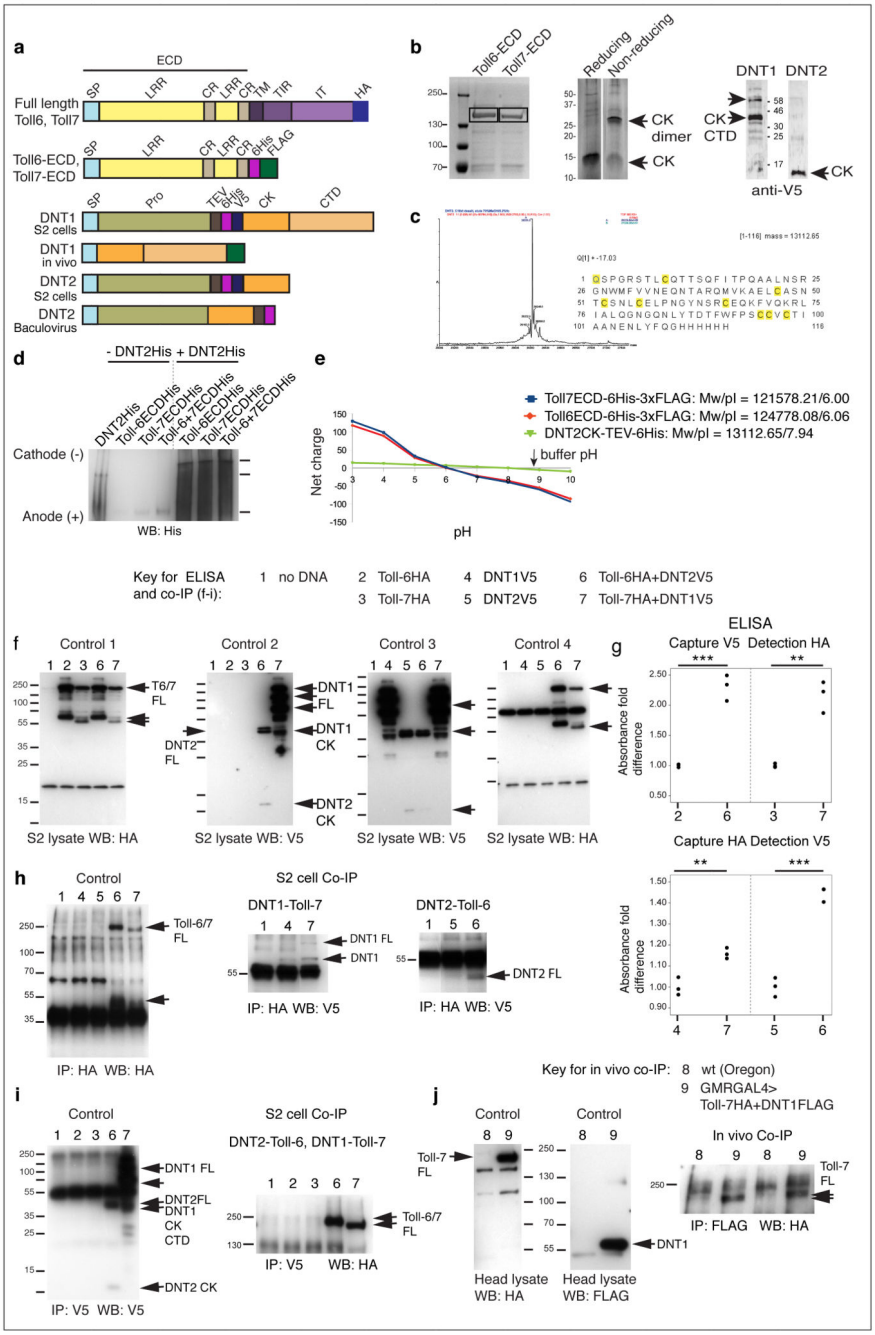

Fig. 6. In vitro, cell culture and in vivo evidence that Toll-7 and Toll-6 bind DNT1 and DNT2

(a) Diagrams illustrating the constructs encoding tagged proteins. (b) Coomassie stainings showing: Left: secreted Toll-6/7ECD purified from S2 cell conditioned medium, for mass spectrometric sequence evidence see Supplementary Fig.5e. Centre: DNT2 is purified from Baculovirus as a secreted cleaved cystine-knot (CK) dimer. Right: DNT1 is purified from S2 conditioned medium as cleaved 45kDa cystine-knot plus terminal extension (CK+CTD, lower arrow), also in full-length (FL) form and cleavage products (upper arrow), and DNT2 is purified from S2 conditioned medium only as cleaved cystine-knot. (c) The mass of

DNT2 purified by reverse phase chromatography determined by MALDI TOF mass spectrometry demonstrates that DNT2 is secreted as a cleaved cystine-knot. The observed mass of the DNT2 dimer was 26225.82±0.62 Da, matching exactly the expected mass. DNT2 is cleaved at a trypsin-like cleavage site. In contrast to Spz, but like vertebrate NGF, DNT2 is processed during biosynthesis. (d) Native gel showing complexes of purified DNT2CK with purified Toll-6ECD, Toll-7ECD or both Toll-6ECD+Toll-7ECD: the shift in the Toll-6/7 band when mixed with DNT2 indicates that these proteins interact (western blot, anti-His). (e) Predicted mobility of native Toll-6ECDHisFLAG, Toll-7ECDHisFLAG and DNT2CKHis at pH=8.8. At this pH the charge of DNT2 is very close to 0, whereas Toll-6 and Toll-7 are negatively charged. (f) Co-transfection S2 cell lysate controls for ELISA and co-IP experiments showing proteins expressed in each experiment in (g,h,i). (g) ELISA assays using co-transfected S2 cells revealed a significant difference in absorbance comparing single and co-transfected S2 cell lysates. Unpaired t-tests: top 6 vs 2: $t(4)=-10.485$ $p<0.001$; 7 vs 3: $t(4)=-7.619$ $p=0.002$; bottom 7 vs 4: $t(4)=-5.574$ $p=0.005$, 6 vs 5: $t(4)=-13.504$ $p<0.001$, n=3 repeats. (h,i) Co-immunoprecipitation of full-length Toll-7HA and DNT1V5, and full-length Toll-6HA and DNT2V5, from co-transfected S2 cells. (h) Precipitation of receptors with anti-HA brings down bound ligands detected with anti-V5; (i) precipitation of ligands with anti-V5 brings down bound receptors detected with anti-HA. (j) In vivo co-immunoprecitation from transgenic flies over-expressing full-length *Toll-7HA* and *DNT1-FLAG* in the retina with *GMRGAL4*. Two examples are shown, using rabbit (left) or mouse (right) anti-FLAG antibodies to precipitate DNT1, bringing down bound receptor detected with anti-HA. ***$p<0.001$, **$p<0.01$, *$p<0.05$. (h, i, j) Co-IP blots have been cropped for clarity; full-length blots are shown in Supplementary Figs.6-9.

Europe PMC Funders Author Manuscripts

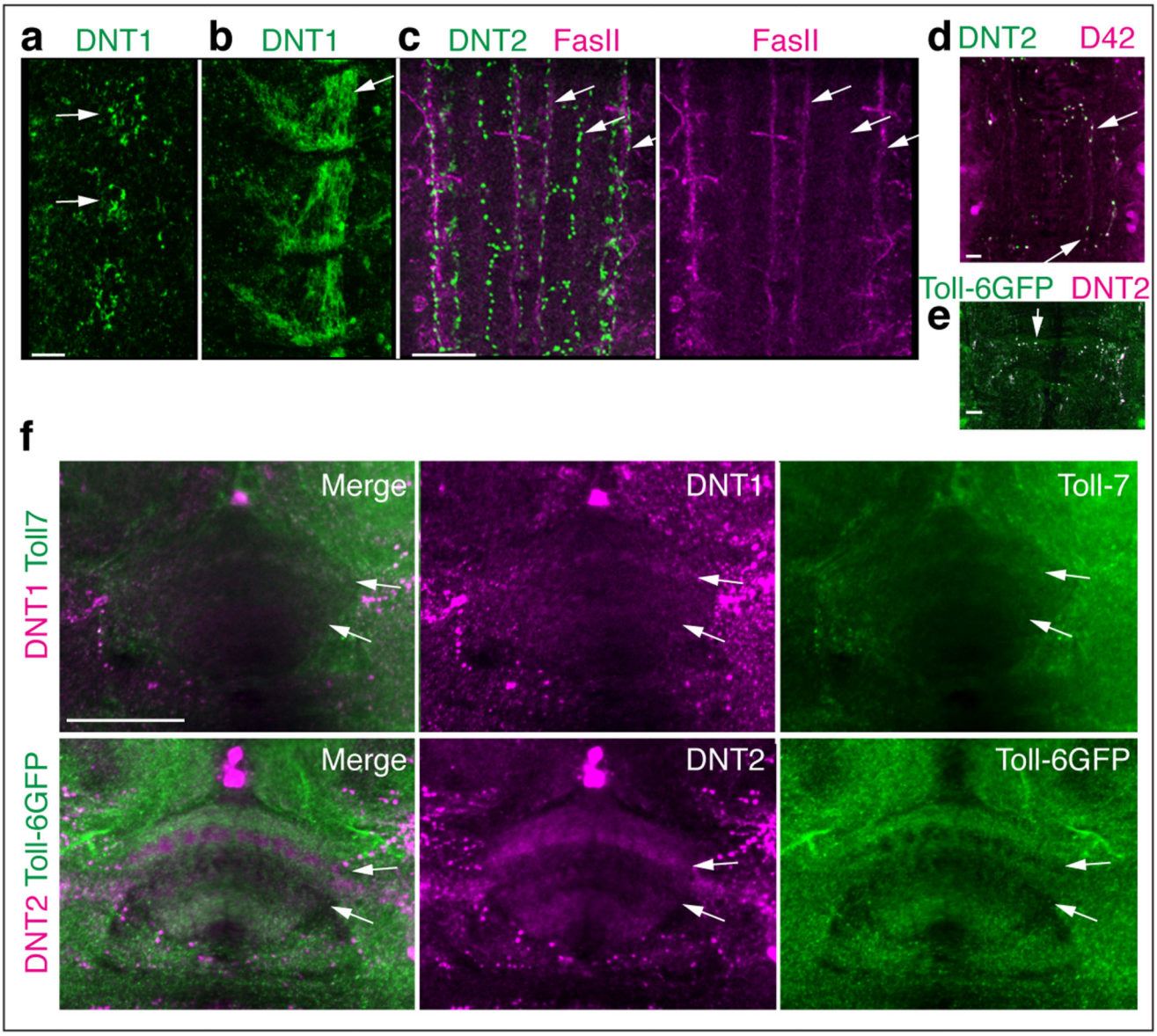

Fig. 7. The relative distributions of DNT1, 2 and Toll-7, 6, respectively, in vivo are consistent with their functions are ligand-receptor pairs

(a) Anti-DNT1 reveals DNT1 protein distributed in the embryonic CNS midline (stage 15) and (b) at high levels in muscle 13,12, in lower levels in muscles 6,7 and possibly others too (stage 17). (c,d) Anti-DNT2 reveals punctate signal along larval CNS axons revealed with (c) FasII+, (d) DsRed+ in Toll-6GAL4(D42)>myrRFP and (e) Toll-$6^{MIMICGFP}$. (f) Anti-DNT1 and anti-Toll-7 co-localise in fan-shaped body layers. Anti-DNT2 and anti-GFP in Toll-$6^{MIMICGFP}$ are distributed in complementary fan-shaped body layers. Anterior is up, scale bar: (a,d,e) 10μm, (c,f) 50μm.